MIT Libraries | DSpace@MIT

MIT Open Access Articles

Search for Dark Matter Produced with an Energetic Jet or a Hadronically Decaying W or Z Boson at √s = 13 TeV

Massachusetts Institute of Technology

Search for dark matter produced with an energetic jet or a hadronically decaying W or Z boson at $\sqrt{s} = 13$ TeV

The CMS collaboration

E-mail: cms-publication-committee-chair@cern.ch

ABSTRACT: A search for dark matter particles is performed using events with large missing transverse momentum, at least one energetic jet, and no leptons, in proton-proton collisions at $\sqrt{s} = 13$ TeV collected with the CMS detector at the LHC. The data sample corresponds to an integrated luminosity of $12.9\,\mathrm{fb}^{-1}$. The search includes events with jets from the hadronic decays of a W or Z boson. The data are found to be in agreement with the predicted background contributions from standard model processes. The results are presented in terms of simplified models in which dark matter particles are produced through interactions involving a vector, axial-vector, scalar, or pseudoscalar mediator. Vector and axial-vector mediator particles with masses up to 1.95 TeV, and scalar and pseudoscalar mediator particles with masses up to 100 and 430 GeV respectively, are excluded at 95% confidence level. The results are also interpreted in terms of the invisible decays of the Higgs boson, yielding an observed (expected) 95% confidence level upper limit of 0.44 (0.56) on the corresponding branching fraction. The results of this search provide the strongest constraints on the dark matter pair production cross section through vector and axial-vector mediators at a particle collider. When compared to the direct detection experiments, the limits obtained from this search provide stronger constraints for dark matter masses less than 5, 9, and 550 GeV, assuming vector, scalar, and axial-vector mediators, respectively. The search yields stronger constraints for dark matter masses less than 200 GeV, assuming a pseudoscalar mediator, when compared to the indirect detection results from Fermi-LAT.

KEYWORDS: Jet substructure, Dark matter, Hadron-Hadron scattering (experiments), Exotics, Higgs physics

Contents

1 Introduction

Astrophysical observations have provided compelling evidence for the existence of dark matter (DM) in the universe [1–3]. However, there is no compelling experimental evidence for non-gravitational interactions between the DM and standard model (SM) particles. Most current models of DM assume that it consists of weakly interacting massive particles (WIMPs) [2]. If such particles exist, direct pair production of WIMPs may occur in TeV-scale collisions at the CERN LHC [4]. If DM particles are produced at the LHC, they would not generate directly observable signals in the detector. However, if they recoil against a jet radiated from the initial state, they may produce an apparent, large transverse momentum imbalance in the event. This is termed the 'monojet' final state [5, 6]. The DM particles may also be produced in association with an electroweak boson, resulting in the 'mono-V' signature, where V represents the W or Z boson [7–9]. Observation of these final states could be interpreted as evidence for DM particles. Additionally, the Higgs boson [10–12] could be a mediator between DM and SM particles [13–17]. The monojet and mono-V signatures can be used to set a bound on the invisible branching fraction of the Higgs boson.

Several previous searches at the LHC have exploited the mono-V and monojet signatures. Results from earlier searches [18–20] have typically been interpreted using effective field theories that model contact interactions between the DM and SM particles. Recent
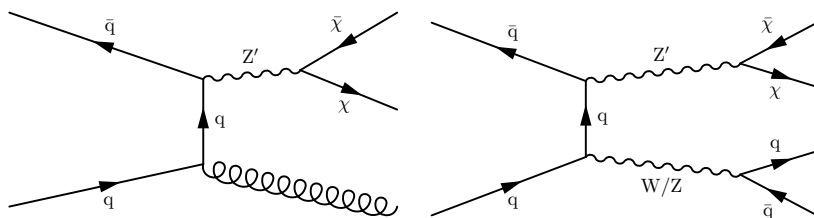
– 1 –

Figure 1. Leading order Feynman diagrams of monojet (left) and mono-V (right) production and decay of a spin-1 mediator.
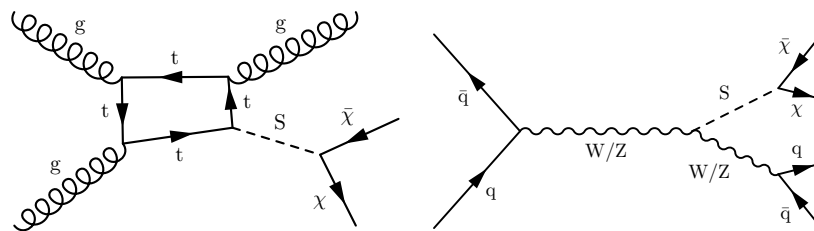

Figure 2. Leading order Feynman diagrams of monojet (left) and mono-V (right) production and decay of a spin-0 mediator.

search results [21–23] have been interpreted in terms of simplified DM models [24–30]. The invisible branching fraction of the Higgs boson, $\mathcal{B}(H \to \text{inv})$, has been constrained by several searches at the LHC [20, 31–34], with the ATLAS and CMS Collaborations setting upper limits of 0.25 and 0.24, at 95% confidence level (CL), respectively, through direct searches [35, 36]. Precise measurements of the Higgs boson couplings from a combination of 7 and 8 TeV data sets, collected by the ATLAS and CMS experiments, provide indirect constraints on additional contributions to the Higgs boson width from non-SM decay processes. The resulting indirect upper limit on the Higgs boson branching fraction to non-SM decays is 0.34, at 95% CL [37].

This paper presents the results of a search for DM in the mono-V and monojet channels using a data set of proton-proton collisions at $\sqrt{s} = 13$ TeV, collected with the CMS detector in the first half of 2016, and corresponding to an integrated luminosity of $12.9\,\text{fb}^{-1}$. In the case of the mono-V signature, a hadronic decay of a W or Z boson reconstructed as a single large-radius jet is considered. The results of the search are interpreted using simplified DM models in which the interaction between the DM and SM particles is mediated by a spin-1 particle such as a Z′ boson, as shown in figure 1, or a spin-0 particle (S), as shown in figure 2. The results are also interpreted in terms of $\mathcal{B}(H \to \text{inv})$. The Feynman diagrams for the production of the SM Higgs boson and its decay to invisible particles resulting in the monojet and mono-V final states are similar to those shown for a spin-0 mediator in figure 2.

2 The CMS detector

The CMS detector is a multi-purpose apparatus designed to study a wide range of physics processes in proton-proton and heavy ion collisions. Its central feature is a superconducting solenoid of 6 m internal diameter that produces a magnetic field of 3.8 T parallel to the beam direction. A silicon pixel and strip tracker is contained inside the solenoid and measures the momentum of charged particles up to a pseudorapidity of $|\eta| = 2.5$. The tracker is surrounded by a lead tungstate crystal electromagnetic calorimeter (ECAL) and a sampling hadron calorimeter (HCAL) made of brass and scintillator, which provide coverage up to $|\eta| = 3$. The steel and quartz-fiber Čerenkov hadron forward calorimeter extends the coverage to $|\eta| = 5$. The muon system consists of gas-ionization detectors embedded in the steel flux-return yoke of the solenoid, and covers $|\eta| < 2.4$. A more detailed description of the CMS detector, together with a definition of the coordinate system used and the relevant kinematic variables, can be found in ref. [38].

The particle-flow (PF) event algorithm [39, 40] reconstructs and identifies each individual particle with an optimized combination of information from the various elements of the CMS detector. The energy of photons is directly obtained from the ECAL measurement. The energy of electrons is determined from a combination of the electron momentum at the primary interaction vertex as determined by the tracker, the energy of the corresponding ECAL cluster, and the energy sum of all bremsstrahlung photons spatially compatible with originating from the electron track. The energy of muons is obtained from the curvature of the corresponding track. The energy of charged hadrons is determined from a combination of their momentum measured in the tracker and the matching ECAL and HCAL energy deposits, corrected for zero-suppression effects and for the response function of the calorimeters to hadronic showers. Finally, the energy of neutral hadrons is obtained from the corresponding ECAL and HCAL energies.

The missing transverse momentum vector ($\vec{p}_\mathrm{T}^\mathrm{miss}$) is computed as the negative vector sum of the transverse momenta (p_T) of all the PF candidates in an event, and its magnitude is denoted as $E_\mathrm{T}^\mathrm{miss}$. Jets are reconstructed by clustering PF candidates using the anti-k_T algorithm [41]. Jets clustered with distance parameters of 0.4 and 0.8 are referred to as AK4 and AK8 jets, respectively. The primary vertex with the largest sum of p_T^2 of the associated tracks is chosen as the vertex corresponding to the hard interaction in an event. All charged PF candidates originating from any other vertex are ignored during the jet reconstruction. Jet momentum is determined as the vectorial sum of all particle momenta in the jet, and is found from simulation to be within 5 to 10% of the true momentum, over the whole p_T spectrum and detector acceptance. An offset correction is applied to jet energies to take into account the contribution from additional proton-proton interactions within the same or adjacent bunch crossings (pileup). Jet energy corrections are derived from simulation and are confirmed with in situ measurements of the energy balance in dijet and γ+jet events [42]. These are also propagated to the $E_\mathrm{T}^\mathrm{miss}$ calculation [43].

3 Event simulation

The Monte Carlo generators used to simulate various signal and background processes are listed in table 1. Simulated samples of background events are produced for the

Z+jets and γ+jets processes at leading order (LO) with up to four partons in the final state, using MadGraph5_aMC@nlo 2.2.3 [44]. This generator is also used to simulate the W($\ell\nu$)+jets process at next-to-leading order (NLO), with up to two partons in the final state, and the quantum chromodynamics (QCD) multijet background at LO. The $t\bar{t}$ and single top quark background samples are produced using Powheg 2.0 [45–47], and a set of diboson samples is produced with Pythia 8.205 [48]. The monojet DM signal is simulated at NLO for spin-1 mediators, and at LO for spin-0 mediators with the resolved top quark loop calculations carried out using Powheg [29, 49]. The mono-V DM signal samples are produced at LO with the JHUGen 5.2.5 generator [50–52] for the scalar mediator, and with MadGraph5_aMC@nlo for the spin-1 mediators. Standard model Higgs boson signal events produced through gluon fusion and vector boson fusion are generated using Powheg, while SM Higgs boson production in association with W or Z bosons is simulated using the JHUGen generator.

Events produced by the MadGraph5_aMC@nlo, Powheg, and JHUGen generators are further processed with Pythia using the CUETP8M1 tune [53] for the simulation of fragmentation, parton shower, hadronization, and the underlying event. In the case of the MadGraph5_aMC@nlo samples, jets from the matrix element calculations are matched to the parton shower description, following the FxFx matching prescription [54] for the NLO samples and the MLM scheme [55] for the LO ones. The NNPDF 3.0 [56] parton distribution functions (PDFs) are used for all generated samples. Interactions of final-state particles with the CMS detector are simulated with Geant4 [57]. Simulated events include the effects of pileup, and are weighted to reproduce the distribution of reconstructed primary vertices observed in data.

4 Event selection

Candidate events are selected using triggers that have thresholds of 90, 100, or 110 GeV applied equally to both $E_{\mathrm{T,trig}}^{\mathrm{miss}}$ and $H_{\mathrm{T,trig}}^{\mathrm{miss}}$, where $E_{\mathrm{T,trig}}^{\mathrm{miss}}$ is computed as the magnitude of the vector sum of the p_{T} of all the particles reconstructed at the trigger level, and $H_{\mathrm{T,trig}}^{\mathrm{miss}}$ is the magnitude of the vector p_{T} sum of jets reconstructed at the trigger level. Jets used in the $H_{\mathrm{T,trig}}^{\mathrm{miss}}$ computation are required to have $p_{\mathrm{T}} > 20\,\mathrm{GeV}$ and $|\eta| < 5.0$. The energy fraction attributed to neutral hadrons in these jets is required to be less than 0.9. This requirement removes jets reconstructed from detector noise. The values of $E_{\mathrm{T,trig}}^{\mathrm{miss}}$ and $H_{\mathrm{T,trig}}^{\mathrm{miss}}$ are calculated without including muon candidates, allowing the same triggers to be used for selecting events in the muon control samples used for background estimation. The trigger efficiency is measured to be about 95% for events passing the analysis selection with $E_{\mathrm{T}}^{\mathrm{miss}} \approx 200\,\mathrm{GeV}$. The triggers become fully efficient for events with $E_{\mathrm{T}}^{\mathrm{miss}} > 350\,\mathrm{GeV}$. Events considered in this search are required to have $E_{\mathrm{T}}^{\mathrm{miss}} > 200\,\mathrm{GeV}$, which ensures that the trigger efficiency is higher than 95%. The leading AK4 jet in the event is required to have $p_{\mathrm{T}} > 100\,\mathrm{GeV}$ and $|\eta| < 2.5$. Unlike earlier searches performed by the CMS Collaboration in this final state [19, 21], there is no requirement on the number of reconstructed jets in the event. The leading AK4 jet must have at least 10% of its energy associated with charged hadrons, and less than 80% of its energy coming from neutral hadrons. These re-

Process	Monte Carlo generator	Perturbative order in QCD
Z+jets	MadGraph5_amc@nlo 2.2.3	LO
γ+jets	MadGraph5_amc@nlo 2.2.3	LO
W+jets	MadGraph5_amc@nlo 2.2.3	NLO
QCD multijet	MadGraph5_amc@nlo 2.2.3	LO
$t\bar{t}$	Powheg 2.0	NLO
Single top quark	Powheg 2.0	NLO
Diboson (ZZ, WZ, WW)	Pythia 8.205	LO
Monojet signal (spin-1 mediator)	Powheg 2.0	NLO
Monojet signal (spin-0 mediator)	Powheg 2.0	LO
Mono-V signal (spin-1 mediator)	MadGraph5_amc@nlo 2.2.3	LO
Mono-V signal (scalar mediator)	JHUGen 5.2.5	LO
H $\to$ inv (gluon fusion)	Powheg 2.0	NLO
H $\to$ inv (vector boson fusion)	Powheg 2.0	NLO
H $\to$ inv (associated production with W or Z)	JHUGen 5.2.5	LO

Table 1. Monte Carlo generators used for simulating various signal and background processes.

quirements, along with quality filters applied to tracks, muon candidates, and other objects, reduce the background due to large misreconstructed E_T^{miss} [43].

The dominant backgrounds in this search are the $Z(\nu\bar{\nu})$+jets and $W(\ell\nu)$+jets processes. The $Z(\nu\bar{\nu})$+jets process constitutes the largest background and is irreducible. The $W(\ell\nu)$+jets background is suppressed by vetoing events that contain at least one isolated electron or muon with $p_T > 10\,\mathrm{GeV}$, or a hadronically decaying τ lepton with $p_T > 18\,\mathrm{GeV}$. Electron candidates must have $|\eta| < 2.5$, and are required to satisfy identification criteria based on the shower shape of the energy deposit in the ECAL, the matching of a track to the ECAL energy cluster, and the consistency of the electron track with the primary vertex [58]. Muon candidates must have $|\eta| < 2.4$, and are required to be identified as muons by the PF algorithm. The isolation sum of the transverse momenta of particles in a cone of radius 0.4 (0.3) around the muon (electron), corrected for the contribution of pileup, is required to be less than 25% (14%) of the muon (electron) transverse momentum. The τ lepton identification criteria [59] require a jet with an identified subset of particles whose invariant mass is consistent with that of a hadronically decaying τ lepton, and for which the pileup-corrected isolation sum of the p_T of particle candidates within a cone of radius 0.3 around the jet axis is less than 5 GeV. Events are vetoed if they contain an isolated photon with $p_T > 15\,\mathrm{GeV}$ that satisfies identification criteria based on its ECAL shower shape [60]. This reduces electroweak backgrounds with a photon radiated from the initial state to about 1% of the total background. The top quark background is suppressed by vetoing events in which a b-jet with $p_T > 15\,\mathrm{GeV}$ is identified using the combined secondary vertex algorithm with the medium working point [61, 62], which has a 60% ef-

ficiency for tagging jets originating from b quarks, and a 1% probability of misidentifying a light-flavor jet as a b-jet. Lastly, in order to suppress the QCD multijet background in which large $E_\mathrm{T}^\mathrm{miss}$ arises from a severe mismeasurement of the jet momenta, the minimum azimuthal angle between $\vec{p}_\mathrm{T}^\mathrm{miss}$ and the directions of each of the four highest p_T AK4 jets with $p_\mathrm{T} > 30\,\mathrm{GeV}$ is required to be greater than 0.5 radians. The QCD multijet background is reduced to about 1% of the total background after this requirement.

After these criteria are applied, events are classified into mono-V or monojet categories. If a V boson has $p_\mathrm{T} > 250\,\mathrm{GeV}$, its hadronic decay is more likely to be reconstructed as a single AK8 jet than as two AK4 jets. An event is categorized as a mono-V event if it has $E_\mathrm{T}^\mathrm{miss} > 250\,\mathrm{GeV}$, and the leading AK8 jet in the event has $p_\mathrm{T} > 250\,\mathrm{GeV}$ and $|\eta| < 2.4$, and also passes requirements used to identify jets arising from hadronic decays of Lorentz-boosted V bosons. Jets arising from hadronic decays of a V boson are identified using the N-subjettiness variable τ_N [63]. Low values of τ_N are indicative of an N-prong decay. In particular, the ratio τ_2/τ_1 discriminates the two-prong decays of a V boson from QCD jets, and the leading AK8 jet is required to have $\tau_2/\tau_1 < 0.6$. Additionally, the invariant mass of the jet is required to be between 65 and 105 GeV in order to be consistent with the mass of the W or Z boson. The jet mass is computed after pruning [64], which involves reclustering of the jet constituents using the Cambridge-Aachen algorithm [65, 66] and removing the soft constituents in every recombination step, thereby improving the jet mass resolution. The requirements on the τ_2/τ_1 ratio and the jet mass result in a 70% efficiency for tagging jets originating from V bosons, and a 5% probability of misidentifying a QCD jet as a V jet. If an event fails any of these mono-V selection requirements, it is assigned to the monojet category. The selection requirements for the mono-V and monojet categories are listed in table 2.

5 Background estimation

The $\mathrm{Z}(\nu\bar{\nu})$+jets and $\mathrm{W}(\ell\nu)$+jets processes constitute about 90% of the total background in this search. These background contributions are estimated using data from dimuon, dielectron, single-muon, single-electron, and γ+jets control samples. Events in each of these control samples are further classified into the monojet and mono-V categories, resulting in ten mutually exclusive control samples. The $E_\mathrm{T}^\mathrm{miss}$ in the control samples is redefined by excluding the leptons and the photons from the calculation. The p_T of the resulting hadronic recoil system resembles the $E_\mathrm{T}^\mathrm{miss}$ distribution of the electroweak backgrounds in the signal region. Therefore, the hadronic recoil p_T is used as a proxy for $E_\mathrm{T}^\mathrm{miss}$ in the control regions.

The dimuon and single-muon events are selected with the same $E_\mathrm{T}^\mathrm{miss}$ triggers that are used to select the signal events. The dimuon events are required to contain exactly two oppositely charged muons, each with $p_\mathrm{T} > 10\,\mathrm{GeV}$. Events are vetoed if there is an additional muon or electron with $p_\mathrm{T} > 10\,\mathrm{GeV}$. At least one of the two muons is required to have $p_\mathrm{T} > 20\,\mathrm{GeV}$ and to pass tight identification requirements based on the number of measurements in the tracker and the muon system, the quality of the muon track fit, and the consistency of the muon track with the primary vertex. The isolation sum of the p_T of particles

Variable	Mono-V requirement	Monojet requirement
E_T^{miss}	> 250 GeV	> 200 GeV
Leading AK4 jet p_T	> 100 GeV	
Leading AK4 jet $|\eta|$	< 2.5	
Charged hadron energy fraction of leading AK4 jet	> 0.1	
Neutral hadron energy fraction of leading AK4 jet	< 0.8	
Number of muons ($p_T > 10$ GeV, $|\eta| < 2.4$)	0	
Number of electrons ($p_T > 10$ GeV, $|\eta| < 2.5$)	0	
Number of τ leptons ($p_T > 18$ GeV, $|\eta| < 2.3$)	0	
Number of photons ($p_T > 15$ GeV, $|\eta| < 2.5$)	0	
Number of b jets ($p_T > 15$ GeV, $|\eta| < 2.4$)	0	
$\Delta\phi$ between four highest p_T jets and E_T^{miss}	> 0.5 radians	
Leading AK8 jet p_T	> 250 GeV	
Leading AK8 jet η	< 2.4	Fails any of the mono-V
Leading AK8 jet τ_2/τ_1	< 0.6	AK8 jet requirements
Leading AK8 jet mass (m_J)	$65 < m_J < 105$ GeV	

Table 2. Selection requirements for the mono-V and monojet event categories.

in a cone of radius 0.4 around the muon, corrected for the contribution of pileup, is required to be less than 15% of the muon p_T. The invariant mass of the dimuon system is required to be between 60 and 120 GeV, in order to be consistent with a Z boson decay. The single-muon events are required to contain exactly one tightly identified and isolated muon with $p_T > 20$ GeV. No additional muon or electron with $p_T > 10$ GeV is allowed, and the transverse mass of the muon-E_T^{miss} system is required to be less than 160 GeV. The transverse mass (m_T) is computed as $m_T^2 = 2E_T^{miss} p_T^\mu (1 - \cos\Delta\phi)$, where p_T^μ is the p_T of the muon, and $\Delta\phi$ is the angle between p_T^μ and $\vec{p}_T^{miss}$. The dimuon and single-muon events are further required to satisfy all other selection requirements imposed on the signal events with the E_T^{miss} replaced by the p_T of the hadronic recoil system. The distribution of the hadronic recoil p_T is then used to estimate the $Z(\nu\bar{\nu})$+jets and $W(\ell\nu)$+jets backgrounds in the signal region.

The dielectron control sample is constructed using events with exactly two oppositely charged electrons with $p_T > 10$ GeV, and no additional muon or electron. The invariant mass of the dielectron system is required to be between 60 and 120 GeV, as in the case of the dimuon events. A single-electron trigger with a p_T threshold of 27 GeV is used to select these events. If the Z boson has $p_T > 600$ GeV, the two electrons produced in its decay typically have a small angular separation, and are likely to be included in each other's isolation cones. This effect results in some inefficiency for the single-electron trigger, which imposes isolation requirements on electron candidates. In order to overcome this inefficiency, events are also accepted if they pass a single-electron trigger that has a p_T threshold of 105 GeV and no isolation requirements on the electron candidate. Furthermore, in order to improve the efficiency of the electron triggers in the early part of the data taking, additional events passing

a trigger with a threshold of $800\,\text{GeV}$ on the total sum of the p_{T} of jets (H_{T}) reconstructed at the trigger level are also included. The same set of triggers is also used for selecting events in the single-electron control sample. At least one of the two electrons in the dielectron control sample is required to have $p_{\mathrm{T}} > 40\,\text{GeV}$, and is required to pass tight identification requirements on the shower shape of its ECAL energy deposit, the matching of a track to the ECAL energy cluster, and the consistency of the electron track with the primary vertex. The isolation sum of the p_{T} of particles in a cone of radius 0.3 around this electron, corrected for the contribution of pileup, is required to be less than 3.5% of the electron p_{T} for electrons within the ECAL barrel ($|\eta| < 1.48$), and less than 6.5% of the electron p_{T} for electrons within the ECAL endcaps ($1.48 < |\eta| < 2.50$). The single-electron events are required to contain exactly one tightly identified and isolated electron with $p_{\mathrm{T}} > 40\,\text{GeV}$. No additional muons or electrons with $p_{\mathrm{T}} > 10\,\text{GeV}$ are allowed. The QCD background in the single-electron control sample is suppressed by requiring $E_{\mathrm{T}}^{\mathrm{miss}} > 50\,\text{GeV}$, and $m_{\mathrm{T}} < 160\,\text{GeV}$.

The γ+jets control sample is constructed using events with one high-p_{T} photon that are selected using single-photon triggers with p_{T} thresholds of 165 or $175\,\text{GeV}$. As in the case of the electron control samples, additional events passing the H_{T} trigger with a threshold of $800\,\text{GeV}$ are also included. The photon p_{T} is required to be larger than $175\,\text{GeV}$, which ensures that the trigger efficiency is greater than 98%. The photon candidate is required to be reconstructed in the ECAL barrel, and is required to pass identification and isolation criteria that ensure an efficiency of 80% in selecting prompt photons, and a sample purity of 95% [60].

The procedure for estimating the $\mathrm{Z}(\nu\bar{\nu})$+jets and $\mathrm{W}(\ell\nu)$+jets backgrounds relies on transfer factors derived from simulation that connect the yields of electroweak processes in the control samples with the background estimates in the signal region, for a given range of $E_{\mathrm{T}}^{\mathrm{miss}}$. The transfer factors for the dilepton control samples relate the yields of $\mathrm{Z}(\mu^+\mu^-)$ and $\mathrm{Z}(\mathrm{e}^+\mathrm{e}^-)$ events to the $\mathrm{Z}(\nu\bar{\nu})$ background in the signal region by taking into account the difference in the branching fractions of $\mathrm{Z}(\nu\bar{\nu})$ and $\mathrm{Z}(\ell^+\ell^-)$ decays and the effect of lepton acceptance and selection efficiencies. In the case of dielectron events these transfer factors also account for the difference in efficiencies of the electron and $E_{\mathrm{T}}^{\mathrm{miss}}$ triggers. The transfer factor for the γ+jets control sample takes into account the difference in the cross sections of the γ+jets and $\mathrm{Z}(\nu\bar{\nu})$+jets processes, the effect of photon acceptance and efficiency, and the difference in the efficiencies of the photon and $E_{\mathrm{T}}^{\mathrm{miss}}$ triggers. Transfer factors are also defined between the $\mathrm{W}(\mu\nu)$ and $\mathrm{W}(\mathrm{e}\nu)$ event yields in the single-lepton control samples and the $\mathrm{W}(\ell\nu)$+jets background estimate in the signal region. These take into account the effect of lepton acceptance, lepton selection efficiencies, τ lepton veto efficiency, and the difference in trigger efficiencies in the case of the single-electron control sample. Finally, a transfer factor is also defined to connect the $\mathrm{Z}(\nu\bar{\nu})$+jets and $\mathrm{W}(\ell\nu)$+jets background yields in the signal region. The photon transfer factor relies on an accurate estimate of the ratio of the γ+jets and Z+jets cross sections. Similarly, the transfer factor between the $\mathrm{Z}(\nu\bar{\nu})$+jets and $\mathrm{W}(\ell\nu)$+jets backgrounds relies on an accurate prediction of the ratio of the W+jets and Z+jets cross sections. Therefore, the LO simulations for the Z+jets and γ+jets processes are corrected using p_{T}-dependent NLO QCD K-factors derived using MadGraph5_amc@nlo, and the Z+jets, W+jets, and γ+jets processes are corrected using p_{T}-dependent NLO electroweak K-factors from theoretical calculations [67–69].

The Z$(\nu\overline{\nu})$+jets and W$(\ell\nu)$+jets background yields are determined through a maximum likelihood fit, performed simultaneously across all the bins of hadronic recoil p_{T} in the ten control samples and $E_{\mathrm{T}}^{\mathrm{miss}}$ in the two signal regions. The likelihood function $\mathcal{L}_k$ for each of the two event categories k, corresponding to the monojet and mono-V selections, is defined as

$$
\begin{aligned}
\mathcal{L}_k(\boldsymbol{\mu}^{\mathrm{Z}(\nu\overline{\nu})}, \boldsymbol{\mu}, \boldsymbol{\theta}) = {} & \prod_i \mathrm{Poisson}\left(d_i^{\gamma} | B_i^{\gamma}(\boldsymbol{\theta}) + \frac{\boldsymbol{\mu}_i^{\mathrm{Z}(\nu\overline{\nu})}}{R_i^{\gamma}(\boldsymbol{\theta})}\right) \\
& \times \prod_i \mathrm{Poisson}\left(d_i^{\mu\mu} | B_i^{\mu\mu}(\boldsymbol{\theta}) + \frac{\boldsymbol{\mu}_i^{\mathrm{Z}(\nu\overline{\nu})}}{R_i^{\mu\mu}(\boldsymbol{\theta})}\right) \\
& \times \prod_i \mathrm{Poisson}\left(d_i^{\mathrm{ee}} | B_i^{\mathrm{ee}}(\boldsymbol{\theta}) + \frac{\boldsymbol{\mu}_i^{\mathrm{Z}(\nu\overline{\nu})}}{R_i^{\mathrm{ee}}(\boldsymbol{\theta})}\right) \\
& \times \prod_i \mathrm{Poisson}\left(d_i^{\mu} | B_i^{\mu}(\boldsymbol{\theta}) + \frac{f_i(\boldsymbol{\theta})\boldsymbol{\mu}_i^{\mathrm{Z}(\nu\overline{\nu})}}{R_i^{\mu}(\boldsymbol{\theta})}\right) \\
& \times \prod_i \mathrm{Poisson}\left(d_i^{\mathrm{e}} | B_i^{\mathrm{e}}(\boldsymbol{\theta}) + \frac{f_i(\boldsymbol{\theta})\boldsymbol{\mu}_i^{\mathrm{Z}(\nu\overline{\nu})}}{R_i^{\mathrm{e}}(\boldsymbol{\theta})}\right) \\
& \times \prod_i \mathrm{Poisson}\left(d_i | B_i(\boldsymbol{\theta}) + (1 + f_i(\boldsymbol{\theta}))\boldsymbol{\mu}_i^{\mathrm{Z}(\nu\overline{\nu})} + \boldsymbol{\mu} S_i(\boldsymbol{\theta})\right)
\end{aligned}
\tag{5.1}
$$

where $\mathrm{Poisson}(x|y) = y^x \mathrm{e}^{-y}/x!$. The symbols $d_i^{\gamma}, d_i^{\mu\mu}, d_i^{\mathrm{ee}}, d_i^{\mu}, d_i^{\mathrm{e}}$, and d_i denote the observed number of events in each bin i of the γ+jets, dimuon, dielectron, single-muon, and single-electron control samples, and the signal region, respectively. The symbol f_i denotes the transfer factor between the Z$(\nu\overline{\nu})$+jets and W$(\ell\nu)$+jets backgrounds in the signal region, and represents a constraint between these backgrounds. The symbols $R_i^{\gamma}, R_i^{\mu\mu}, R_i^{\mathrm{ee}}, R_i^{\mu}$, and R_i^{e} are the transfer factors from the γ+jets, dimuon, dielectron, single-muon, and single-electron control samples, respectively, to the signal region; the contributions from other background processes in these control samples are denoted by $B_i^{\gamma}, B_i^{\mu\mu}, B_i^{\mathrm{ee}}, B_i^{\mu}$, and B_i^{e}, respectively. The parameter $\boldsymbol{\mu}_i^{\mathrm{Z}(\nu\overline{\nu})}$ represents the yield of the Z$(\nu\overline{\nu})$+jets background in each bin i of $E_{\mathrm{T}}^{\mathrm{miss}}$ in the signal region, and this parameter is left floating in the fit. The likelihood also includes a term for the signal region in which B_i represents all the backgrounds apart from Z$(\nu\overline{\nu})$+jets and W$(\ell\nu)$+jets, S_i represents the nominal signal prediction, and $\boldsymbol{\mu}$ denotes the signal strength parameter. The systematic uncertainties are modeled as nuisance parameters ($\boldsymbol{\theta}$).

The uncertainties in the Z$(\nu\overline{\nu})$+jets and W$(\ell\nu)$+jets backgrounds enter the likelihood as constrained perturbations of the transfer factors $R_i^{\gamma}, R_i^{\mu\mu}, R_i^{\mathrm{ee}}, R_i^{\mu}, R_i^{\mathrm{e}}$ and f_i. These include theoretical uncertainties in the γ+jets to Z+jets, and W+jets to Z+jets differential cross section ratios from the choice of the renormalization (10–15%) and factorization (1–10%) scales [21], and the PDF modeling uncertainty, which is found to be negligible. The effect of missing higher-order electroweak corrections to the γ+jets, W+jets, and Z+jets processes is covered by propagating the full NLO electroweak correction as a function of the boson p_{T} as the uncertainty. The resulting uncertainty varies within 2–14%
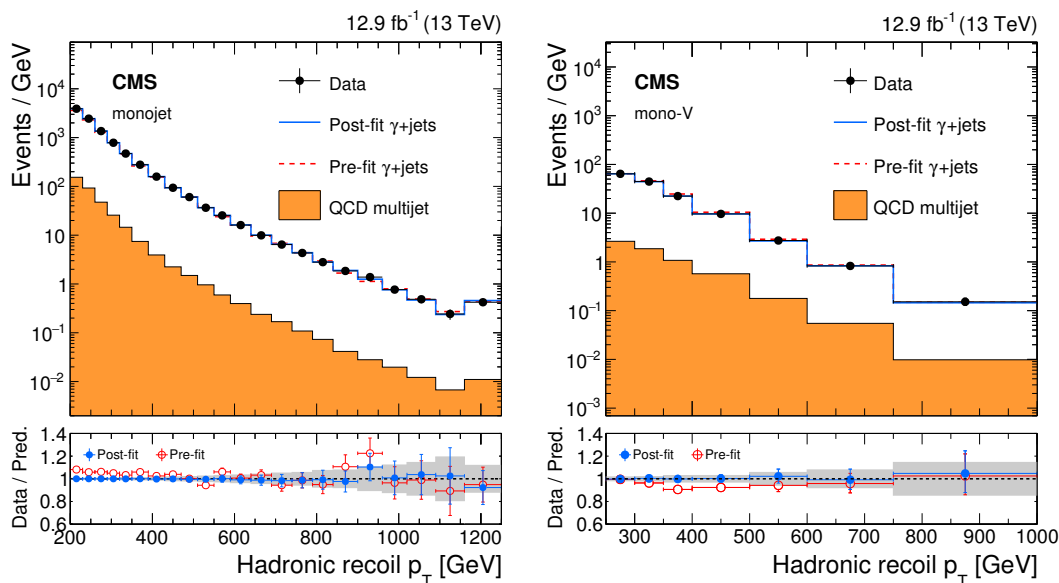
Figure 3. Comparison between data and Monte Carlo simulation in the γ+jets control sample before and after performing the simultaneous fit across all the control samples and the signal region, assuming the absence of any signal. The left plot shows the monojet category and the right plot shows the mono-V category. The hadronic recoil p_T in γ+jets events is used as a proxy for E_T^{miss} in the signal region. The filled histogram indicates the multijet background. Ratios of data and the pre-fit background prediction (red points) and post-fit background prediction (blue points) are shown for both the monojet and mono-V signal categories. The gray band indicates the overall post-fit uncertainty. The last bin includes all events with hadronic recoil p_T larger than 1160 (750) GeV in the monojet (mono-V) category.

and 1–9% for the γ+jets to Z+jets and W+jets to Z+jets differential cross section ratios, respectively, and it is conservatively considered to be uncorrelated across the bins of hadronic recoil p_T. Uncertainties in the reconstruction efficiencies of leptons (1% per muon or electron); in selection efficiencies of leptons (2% per muon or electron), photons (2%), and hadronically decaying τ leptons (3%); in the purity of photons in the γ+jets control sample (2%); and in the efficiency of the electron (2%), photon (2%), and E_T^{miss} (1%) triggers, are included and their correlations across all the bins of hadronic recoil p_T are taken into account. Figures 3–5 show the results of the combined fit in the ten control samples and the two signal regions assuming the absence of any signal. Data in the control samples are compared to the pre-fit predictions from simulation and the post-fit estimates obtained after performing the fit. The control samples with larger yields dominate the fit results.

In addition to the $Z(\nu\overline{\nu})$+jets and $W(\ell\nu)$+jets processes, several other sources of background contribute to the total event yield in the signal region. These include QCD multijet events that have little genuine E_T^{miss}. However, jet mismeasurement and instrumental effects can give rise to high E_T^{miss} tails. A $\Delta\phi$ extrapolation method [70] is used to estimate this background. In this method, a background-enriched control sample is obtained by selecting events that fail the $\Delta\phi$ requirement between jets and E_T^{miss}, but pass the remaining
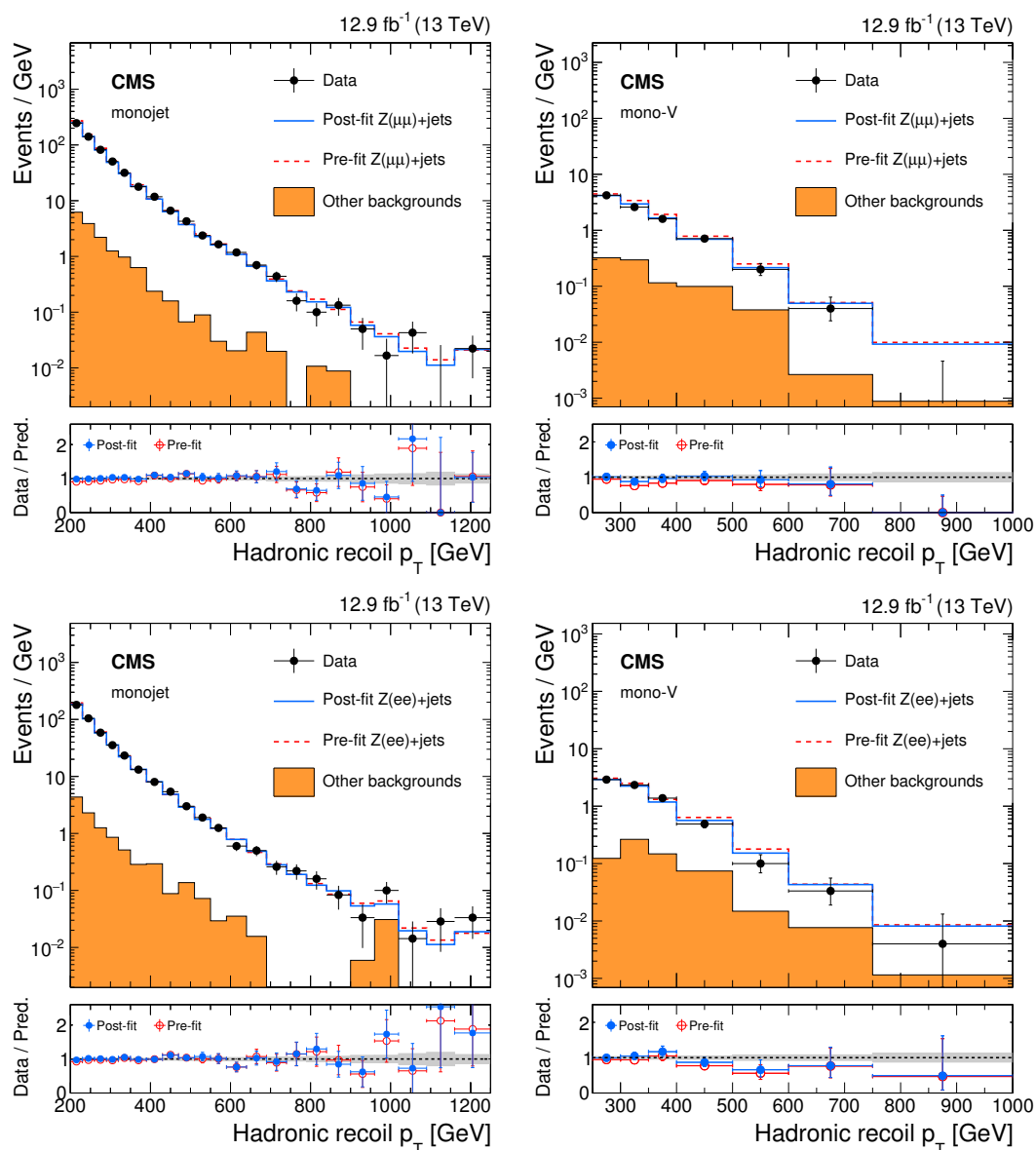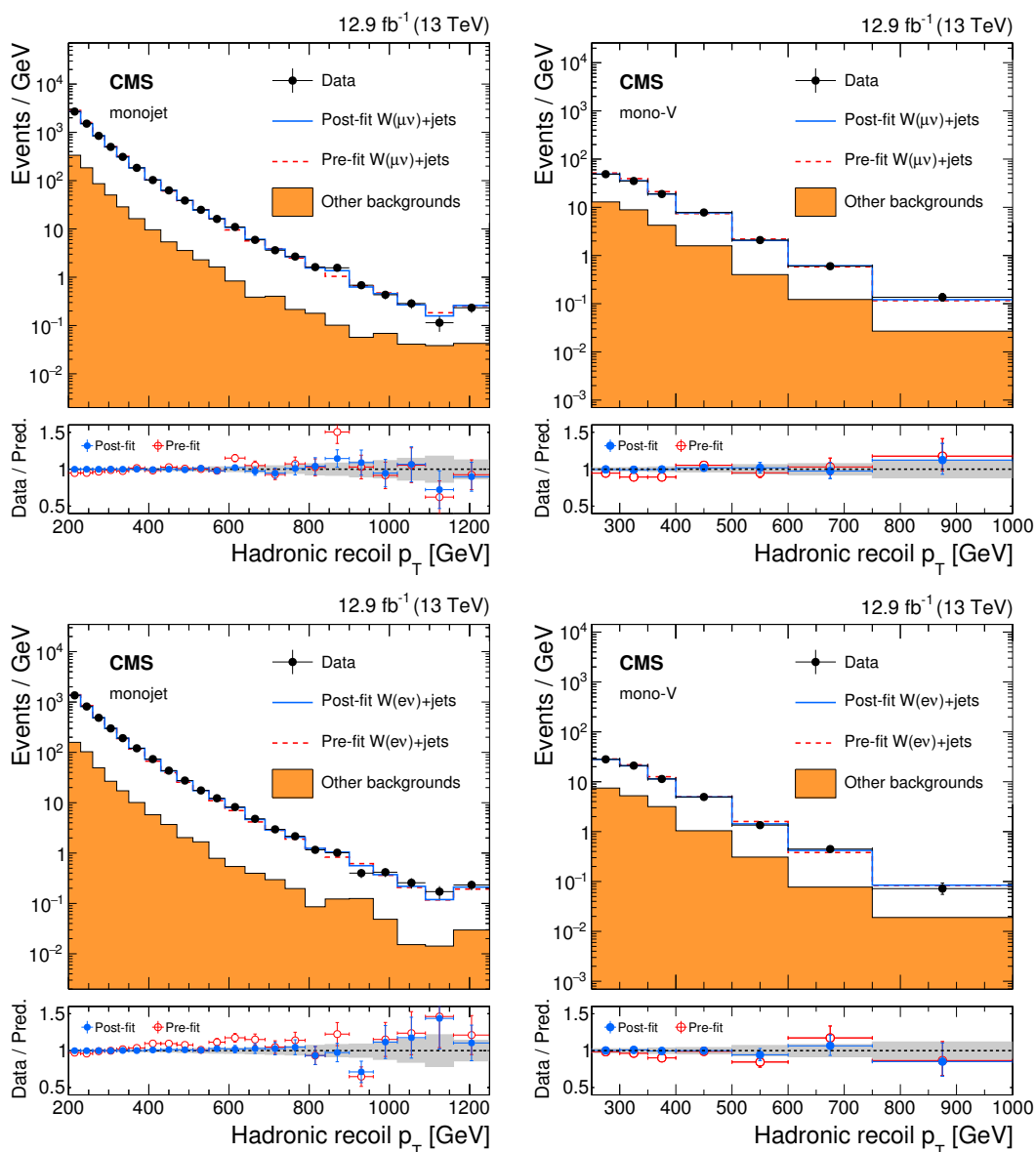
Figure 4. Comparison between data and Monte Carlo simulation in the dilepton control samples before and after performing the simultaneous fit across all the control samples and the signal region, assuming the absence of any signal. Plots on the upper left and right correspond to the monojet and mono-V categories, respectively, in the dimuon control sample. Plots on the bottom left and right correspond to the monojet and mono-V categories, respectively, in the dielectron control sample. The hadronic recoil p_T in dilepton events is used as a proxy for E_T^{miss} in the signal region. The filled histogram indicates all processes other than $Z(\ell^+\ell^-)$+jets. Ratios of data and the pre-fit background prediction (red points) and post-fit background prediction (blue points) are shown for both the monojet and mono-V signal categories. The gray band indicates the overall post-fit uncertainty. The last bin includes all events with hadronic recoil p_T larger than 1160 (750) GeV in the monojet (mono-V) category.

Figure 5. Comparison between data and Monte Carlo simulation in the single-lepton control samples before and after performing the simultaneous fit across all the control samples and the signal region, assuming the absence of any signal. Plots on the upper left and right correspond to the monojet and mono-V categories, respectively, in the single-muon control sample. Plots on the bottom left and right correspond to the monojet and mono-V categories, respectively, in the single-electron control sample. The hadronic recoil p_T in single-lepton events is used as a proxy for E_T^{miss} in the signal region. The filled histogram indicates all processes other than $W(\ell\nu)$+jets. Ratios of data and the pre-fit background prediction (red points) and post-fit background prediction (blue points) are shown for both the monojet and mono-V signal categories. The gray band indicates the overall post-fit uncertainty. The last bin includes all events with hadronic recoil p_T larger than 1160 (750) GeV in the monojet (mono-V) category.

event selection criteria. An estimate of the multijet background in the signal region is obtained by applying E_T^{miss}-dependent transfer factors, derived from simulated QCD multijet events, to this control sample. The overall uncertainty in the multijet background estimate, based on the variations of the jet response and the statistical uncertainties in the transfer factors, ranges from 50 to 150%, depending on the event category and the E_T^{miss} region.

The remaining background sources include top quark and diboson processes, which are estimated directly from simulation. The p_T distribution of the top quark in simulation is corrected to match the observed p_T distribution in data [71]. A systematic uncertainty of 10% is assigned to the prediction of the top quark background cross section [72]. An additional 10% uncertainty is assigned to the top quark background normalization to take account of the modeling of the top quark p_T distribution in simulation. The overall normalization of the diboson background has an uncertainty of 20% [73, 74]. These uncertainties in the top quark and diboson backgrounds are correlated across the signal and control samples. Several experimental sources of uncertainty are associated with the backgrounds estimated from simulation. An uncertainty of 6.2% in the integrated luminosity measurement [75] is propagated to the background yields. The uncertainty in the efficiency of the b-jet veto is estimated to be 6% for the top quark background and 2% for the diboson background. The uncertainty in the efficiency of the V tagging requirements is estimated to be 13% in the mono-V category. The uncertainty in the modeling of E_T^{miss} in simulation [76] is dominated by the jet energy scale uncertainty, and is estimated to be 5%.

6 Results and interpretation

Figure 6 shows the E_T^{miss} distributions in the monojet and mono-V signal regions. The background prediction is obtained from a combined fit in all the control samples, excluding the signal region. Data are found to be in agreement with the SM prediction. Tables 3 and 4 show the estimated yields of background processes in the monojet and mono-V signal regions, respectively, along with the observed event yields in the two signal regions. The correlations between the uncertainties across all the E_T^{miss} bins in the two signal regions are reported in appendix A. These results can be used with the simplified likelihood approach detailed in ref. [77] for reinterpretations in terms of models not studied in this paper.

Figure 7 shows the E_T^{miss} distributions where the background estimates have been computed after including events from the signal region in the fit, but assuming the absence of any signal. The comparison of this fit with an alternative fit assuming the presence of signal is used to set limits on the DM signal cross section.

6.1 Dark matter interpretation

The results of the search are interpreted in terms of simplified DM models for the monojet and mono-V final states, assuming a vector, axial-vector, scalar, or pseudoscalar mediator decaying into a pair of fermionic DM particles. These results supersede those from the earlier CMS publications in the same final states [19, 21].

The mediators are assumed to interact with the pair of DM particles with coupling strength $g_{DM} = 1$. The spin-1 mediators are assumed to interact with SM quarks with

E_T^{miss} [GeV]	Z($\nu\bar{\nu}$)+jets	W($\ell\nu$)+jets	Top quark	Dibosons	Other	Total bkg.	Observed
200–230	71300 ± 2200	54600 ± 2300	2140 ± 320	1320 ± 220	2470 ± 310	132100 ± 4000	140642
230–260	39500 ± 1300	27500 ± 1200	1060 ± 160	790 ± 130	1090 ± 130	69900 ± 2200	73114
260–290	21900 ± 670	13600 ± 550	440 ± 65	364 ± 61	498 ± 65	36800 ± 1100	38321
290–320	12900 ± 400	7300 ± 290	210 ± 31	235 ± 40	216 ± 30	20780 ± 630	21417
320–350	8000 ± 280	4000 ± 170	107 ± 16	145 ± 24	124 ± 18	12340 ± 400	12525
350–390	6100 ± 220	2800 ± 130	74 ± 11	111 ± 19	87 ± 13	9160 ± 320	9515
390–430	3500 ± 160	1434 ± 66	30.1 ± 4.5	58.4 ± 9.9	33.4 ± 5.3	5100 ± 200	5174
430–470	2100 ± 98	816 ± 37	16.6 ± 2.5	42.4 ± 7.1	16.3 ± 2.7	3000 ± 120	2947
470–510	1300 ± 66	450 ± 20	7.4 ± 1.1	24.6 ± 4.1	9.6 ± 1.6	1763 ± 79	1777
510–550	735 ± 39	266 ± 13	5.2 ± 0.8	18.5 ± 3.1	7.0 ± 1.3	1032 ± 48	1021
550–590	513 ± 31	152 ± 8	2.4 ± 0.4	13.5 ± 2.3	1.1 ± 0.3	683 ± 37	694
590–640	419 ± 23	120 ± 6	1.5 ± 0.2	10.6 ± 1.8	2.1 ± 0.4	554 ± 28	554
640–690	246 ± 16	62.8 ± 3.8	1.3 ± 0.2	11.4 ± 1.9	1.0 ± 0.2	322 ± 19	339
690–740	139 ± 11	34.2 ± 2.4	0.6 ± 0.1	4.2 ± 0.7	0.20 ± 0.07	178 ± 13	196
740–790	97.2 ± 7.2	22.7 ± 1.7	0.22 ± 0.03	1.4 ± 0.2	0.63 ± 0.12	122 ± 8	123
790–840	59.8 ± 5.8	12.9 ± 1.2	0.13 ± 0.02	1.5 ± 0.3	0.05 ± 0.02	74.5 ± 6.6	80
840–900	64.3 ± 6.4	12.3 ± 1.1	0.24 ± 0.04	0.92 ± 0.1	0.03 ± 0.01	77.8 ± 7.2	68
900–960	31.5 ± 4.3	6.0 ± 0.7	0.21 ± 0.03	0.74 ± 0.1	0.01 ± 0.01	38.4 ± 4.8	37
960–1020	20.8 ± 3.0	3.4 ± 0.5	—	0.94 ± 0.2	0.01 ± 0.01	25.1 ± 3.4	23
1020–1090	16.3 ± 2.6	3.1 ± 0.5	0.04 ± 0.01	1.6 ± 0.3	0.01 ± 0.01	21.1 ± 3.0	12
1090–1160	8.1 ± 1.8	1.3 ± 0.3	—	—	—	9.4 ± 1.9	7
>1160	18.6 ± 2.7	2.7 ± 0.4	—	1.3 ± 0.2	—	22.6 ± 3.0	26

Table 3. Expected event yields in each E_T^{miss} bin for various background processes in the monojet signal region. The background yields and the corresponding uncertainties are obtained after performing a combined fit to data in all the control samples, but excluding data in the signal region. The observed event yields in the monojet signal region are also reported.

E_T^{miss} [GeV]	Z($\nu\bar{\nu}$)+jets	W($\ell\nu$)+jets	Top quark	Dibosons	Other	Total bkg.	Observed
250–300	1700 ± 88	1100 ± 65	171 ± 24	195 ± 35	49.4 ± 10.8	3220 ± 130	3395
300–350	1180 ± 68	627 ± 37	68.8 ± 9.7	135 ± 24	44.2 ± 7.2	2050 ± 88	2162
350–400	629 ± 37	314 ± 21	28.9 ± 4.1	68.5 ± 12	8.0 ± 1.8	1048 ± 51	1093
400–500	500 ± 33	181 ± 13	21.4 ± 3.0	62.8 ± 11	10.1 ± 1.8	775 ± 40	780
500–600	131 ± 12	38.5 ± 3.4	2.9 ± 0.4	16.8 ± 3.0	4.1 ± 0.8	193 ± 14	207
600–750	57.1 ± 5.9	15.6 ± 1.6	1.0 ± 0.1	9.8 ± 1.7	0.8 ± 0.1	84.2 ± 6.9	90
>750	16.5 ± 2.7	3.6 ± 0.6	—	4.7 ± 0.8	0.01 ± 0.01	24.8 ± 3.1	27

Table 4. Expected event yields in each E_T^{miss} bin for various background processes in the mono-V signal region. The background yields and the corresponding uncertainties are obtained after performing a combined fit to data in all the control samples, excluding data in the signal region. The observed event yields in the mono-V signal region are also reported.
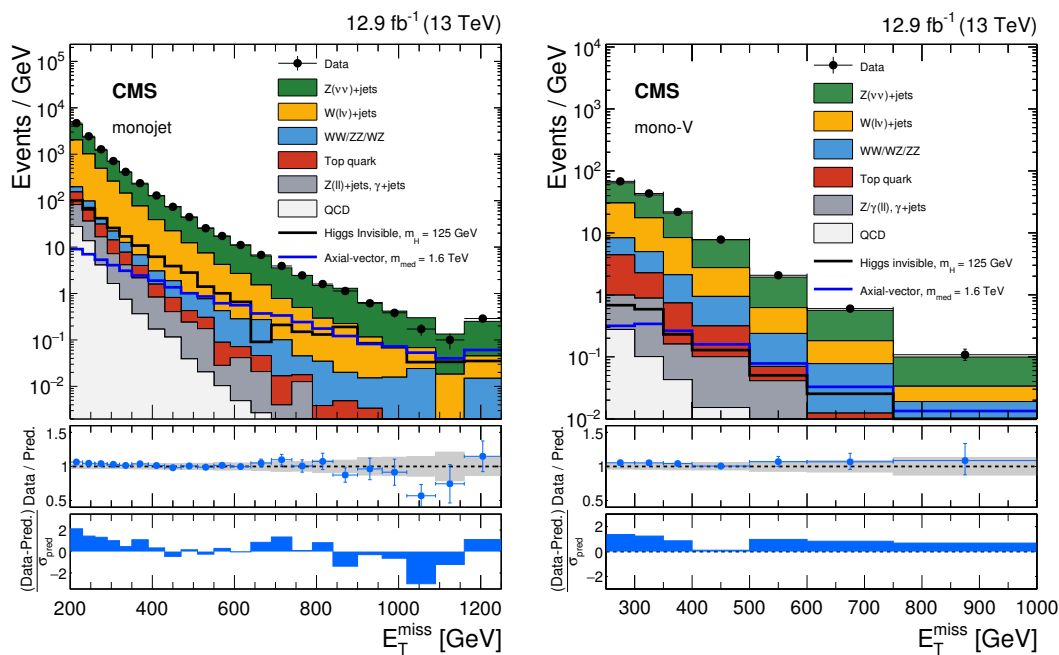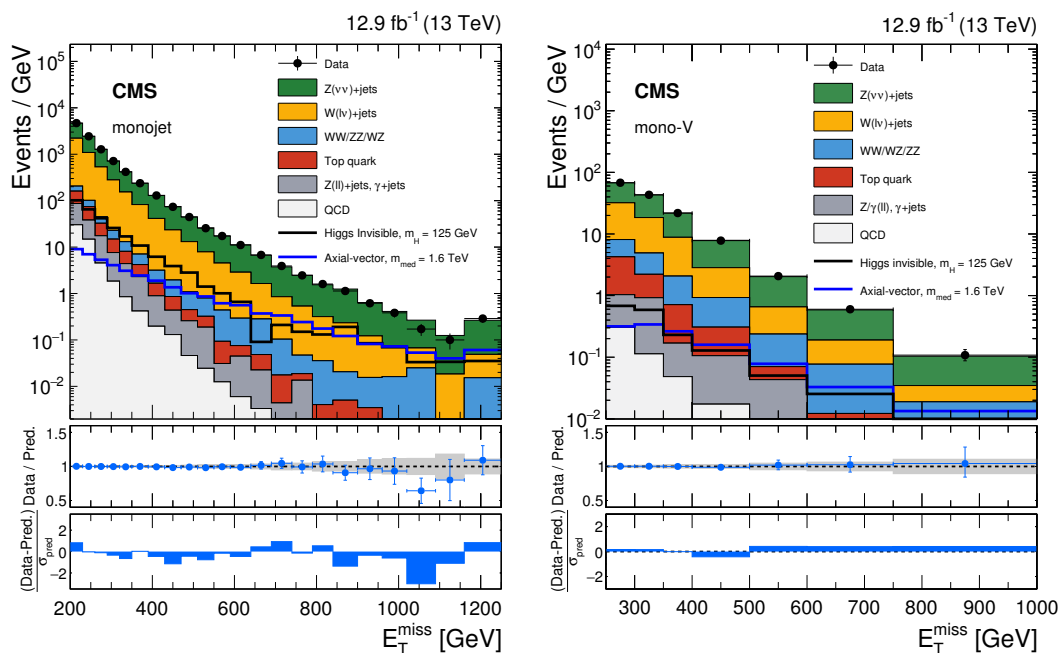
Figure 6. Observed E_T^{miss} distribution in the monojet (left) and mono-V (right) signal regions compared with the background expectations for various SM processes evaluated after performing a combined fit to the data in all the control samples, but excluding the signal region. The last bin includes all events with $E_T^{miss} > 1160\,(750)$ GeV for the monojet (mono-V) category. Expected signal distributions for a 125 GeV Higgs boson decaying exclusively to invisible particles, and for a 1.6 TeV axial-vector mediator decaying to 1 GeV DM particles, are overlaid. The ratio of data and the post-fit background prediction is shown for both the monojet and mono-V signal regions. The gray bands in these ratio plots indicate the post-fit uncertainty in the background prediction. Finally, the distributions of the pulls, defined as the difference between data and the post-fit background prediction relative to the post-fit uncertainty in the prediction, are also shown in the lower panels.

coupling strength $g_q = 0.25$. The spin-0 mediators are assumed to couple to the quarks through SM-like Yukawa interactions with the coupling strength modifier $g_q = 1$. The width of the mediators is determined assuming they interact only with the SM particles and the DM particle. The choice of all the signal model parameters follows the recommendations from ref. [78] (section 2.1 and 2.2). Uncertainties of 20 and 30% are assigned to the inclusive signal cross section in the case of the spin-1 and spin-0 mediators, respectively. These include the renormalization and factorization scale uncertainties, and the PDF uncertainty.

Upper limits are computed at 95% CL on the ratio of the signal cross section to the predicted cross section, denoted by $\mu = \sigma/\sigma_{th}$, with the CL_s method [79, 80], using the asymptotic approximation [81]. Limits are obtained as a function of the mediator mass, m_{med}, and the DM mass, m_{DM}. In the case of the vector, axial-vector and scalar mediators, limits are computed on the combined cross section due to the monojet and mono-V signal processes. In the case of the pseudoscalar mediator, limits are computed assuming only the monojet signal process. The mono-V signal process (figure 2, right), in which

Figure 7. Observed E_T^{miss} distribution in the monojet (left) and mono-V (right) signal regions compared with the background expectations for various SM processes evaluated after performing a combined fit to the data in all the control samples, as well as in the signal region. The fit is performed assuming the absence of any signal. The last bin includes all events with $E_T^{miss} > 1160$ (750) GeV for the monojet (mono-V) category. Expected signal distributions for a 125 GeV Higgs boson decaying exclusively to invisible particles, and for a 1.6 TeV axial-vector mediator decaying to 1 GeV DM particles, are overlaid. The ratio of data and the post-fit background prediction is shown for both the monojet and mono-V signal regions. The gray bands in these ratio plots indicate the post-fit uncertainty in the background prediction. Finally, the distributions of the pulls, defined as the difference between data and the post-fit background prediction relative to the post-fit uncertainty in the prediction, are also shown in the lower panels.

a pseudoscalar mediator couples directly to vector bosons, is ill-defined without making additional assumptions [82] and therefore is not included. Figure 8 shows the exclusion contours in the m_{med}-m_{DM} plane for the vector and axial-vector mediators. Mediator masses up to 1.95 TeV and DM masses up to 750 and 550 GeV are excluded for the vector and axial-vector models, respectively, at 95% CL. Figure 9 shows the exclusion contours in the m_{med}-m_{DM} plane for the scalar and pseudoscalar mediators. For scalar mediators, masses up to 100 GeV and DM masses up to 35 GeV are excluded at 95% CL, and no exclusion is expected or observed considering only the monojet signal process. Pseudoscalar mediator masses up to 430 GeV and DM masses up to 170 GeV are excluded at 95% CL. Figure 10 shows the limits for the spin-0 models as a function of the mediator mass, assuming the DM mass to be 1 GeV. In the case of the scalar mediator limits are computed for the monojet signal process, and for the combination of the monojet and mono-V signal processes.

Figures 8 and 9 also show the constraints from the observed cosmological relic density of DM as determined from measurements of the cosmic microwave background by the Planck satellite experiment [83]. The expected DM abundance is estimated using the
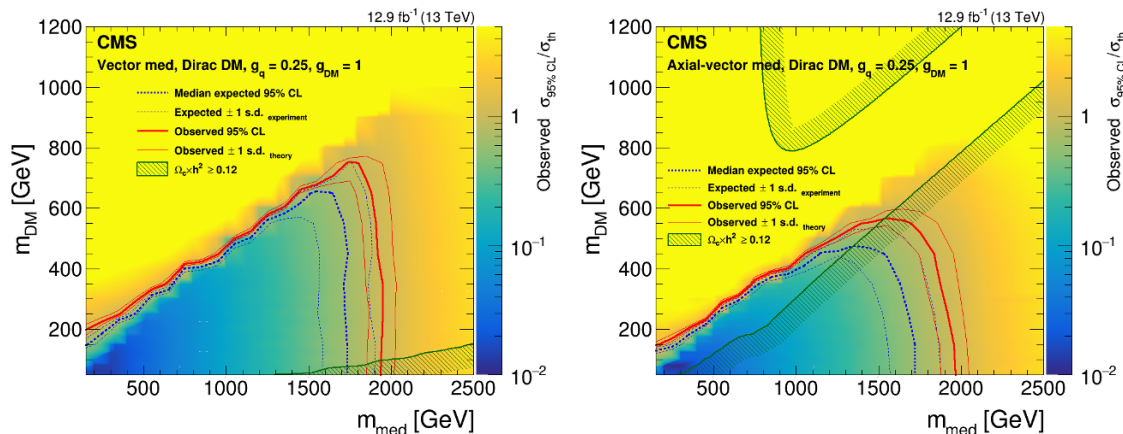
Figure 8. Exclusion limits at 95% CL on the signal strength $\mu = \sigma/\sigma_{\rm th}$ in the $m_{\rm med}$-$m_{\rm DM}$ plane assuming vector (left) and axial-vector (right) mediators. The limits are shown for $m_{\rm med}$ between 150 GeV and 2.5 TeV, and $m_{\rm DM}$ between 50 GeV and 1.2 TeV. While the excluded area is expected to extend below these minimum values of $m_{\rm med}$ and $m_{\rm DM}$, the axes do not extend below these values as the signal simulation was not performed in this region. The solid (dotted) red (blue) line shows the contour for the observed (expected) exclusion. The solid contours around the observed limit and the dashed contours around the expected limit represent one standard deviation theoretical uncertainties in the signal cross section and the combination of the statistical and experimental systematic uncertainties, respectively. Constraints from the Planck satellite experiment [83] are shown with the dark green contours and associated hatching. The hatched area indicates the region where the DM density exceeds the observed value.

thermal freeze-out mechanism implemented in the MADDM [84] package, and compared to the observed cold DM density $\Omega_c h^2 = 0.12$ [85], where Ω_c is the DM relic abundance and h is the Hubble constant, under the assumption that a single DM particle describes DM interactions in the early universe and that this particle only interacts with SM particles through the considered simplified model [86, 87].

The limits obtained using the simplified DM models may be compared to the results from direct and indirect DM detection experiments, which are usually expressed as 90% CL upper limits on the DM-nucleon scattering cross sections. The approach outlined in refs. [30, 88, 89] is used to translate the exclusion contours into the $m_{\rm DM}$ vs. $\sigma_{\rm SI/SD}$ plane where $\sigma_{\rm SI/SD}$ are the spin-independent/spin-dependent DM-nucleon scattering cross sections. These limits are shown in figure 11 for the vector and axial-vector mediators, and in figure 12 (left) for the scalar mediator. For the scalar mediator model, only the contributions from heavy quarks (charm, bottom, and top) are taken into account while evaluating the limit on the DM-nucleon cross section, as done in ref. [21]. When compared to the results from direct detection experiments, the limits obtained from this search provide stronger constraints for dark matter masses less than 5, 9, and 550 GeV, assuming vector, scalar, and axial-vector mediators, respectively. In the case of the pseudoscalar mediator, the 95% CL upper limits are compared in figure 12 (right) with the indirect detection results in terms of the velocity-averaged DM annihilation cross section from the Fermi-LAT Collaboration [90], and provide stronger constraints for DM masses less than 200 GeV.
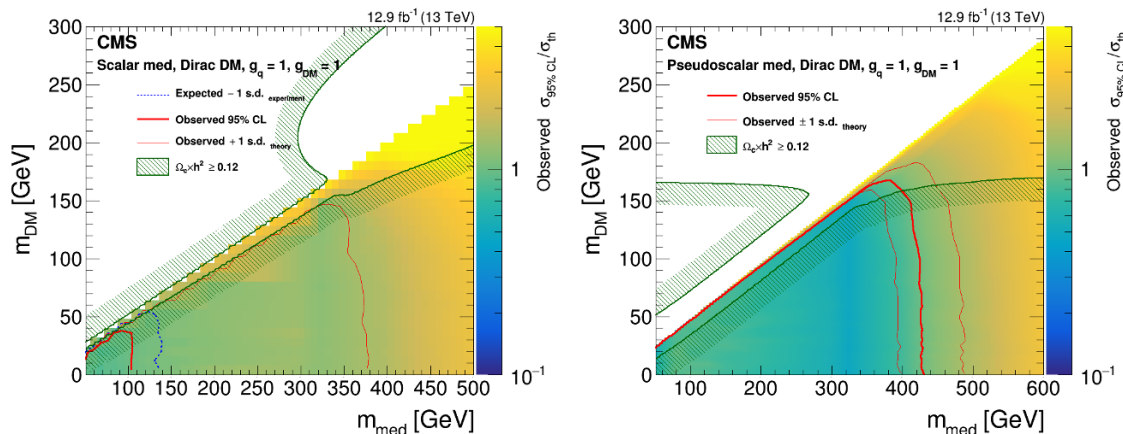
Figure 9. Exclusion limits at 95% CL on signal strength the $\mu = \sigma/\sigma_{\text{th}}$ in the m_{med}-m_{DM} plane assuming scalar (left) and pseudoscalar (right) mediators. The limits are shown for m_{med} between 50 and 500 GeV, and m_{DM} between 0 and 300 GeV. While the excluded area is expected to extend below the minimum value of m_{med}, the axis does not extend below this value as the signal simulation was not performed in this region. The red line shows the contour for the observed exclusion. The solid red contours around the observed limit represent one standard deviation theoretical uncertainties in the signal cross section. The dashed blue contour in the case of the scalar mediator shows the -1σ deviation due to the combination of the statistical and experimental systematic uncertainties. Constraints from the Planck satellite experiment [83] are shown with the dark green contours and associated hatching. The hatched area indicates the region where the DM density exceeds the observed value.

6.2 Invisible decays of the Higgs boson

The results of this search are also interpreted in terms of an upper limit on the product of the cross section and branching fraction $\mathcal{B}(\text{H} \to \text{inv})$, relative to the predicted cross section (σ_{SM}) of the Higgs boson assuming SM interactions, where the Higgs boson is produced through gluon fusion (ggH) along with a jet; in association with a vector boson (ZH, WH); or through vector boson fusion (VBF). The predictions for the Higgs boson production cross section and the corresponding theoretical uncertainties are taken from the recommendations of the LHC Higgs cross section working group [101]. If the production cross section of the Higgs boson is assumed to be the same as σ_{SM}, this limit can be used to constrain the invisible branching fraction of the Higgs boson. The observed (expected) 95% CL upper limit on the invisible branching fraction of the Higgs boson, $\sigma\mathcal{B}(\text{H} \to \text{inv})/\sigma_{\text{SM}}$, is found to be 0.44 (0.56). The limits are summarized in figure 13. Table 5 shows the individual limits for the monojet and mono-V categories. While these limits on $\mathcal{B}(\text{H} \to \text{inv})$ are not as strong as the combined ones from ref. [36], they are obtained from an independent data sample and therefore will contribute to future combinations.

7 Summary

A search for dark matter (DM) is presented using events with jets and large missing transverse momentum in a $\sqrt{s} = 13\,\text{TeV}$ proton-proton collision data set corresponding to an integrated luminosity of $12.9\,\text{fb}^{-1}$. The search also exploits events with a hadronic decay of a W or Z boson reconstructed as a single large-radius jet. No significant excess is ob-
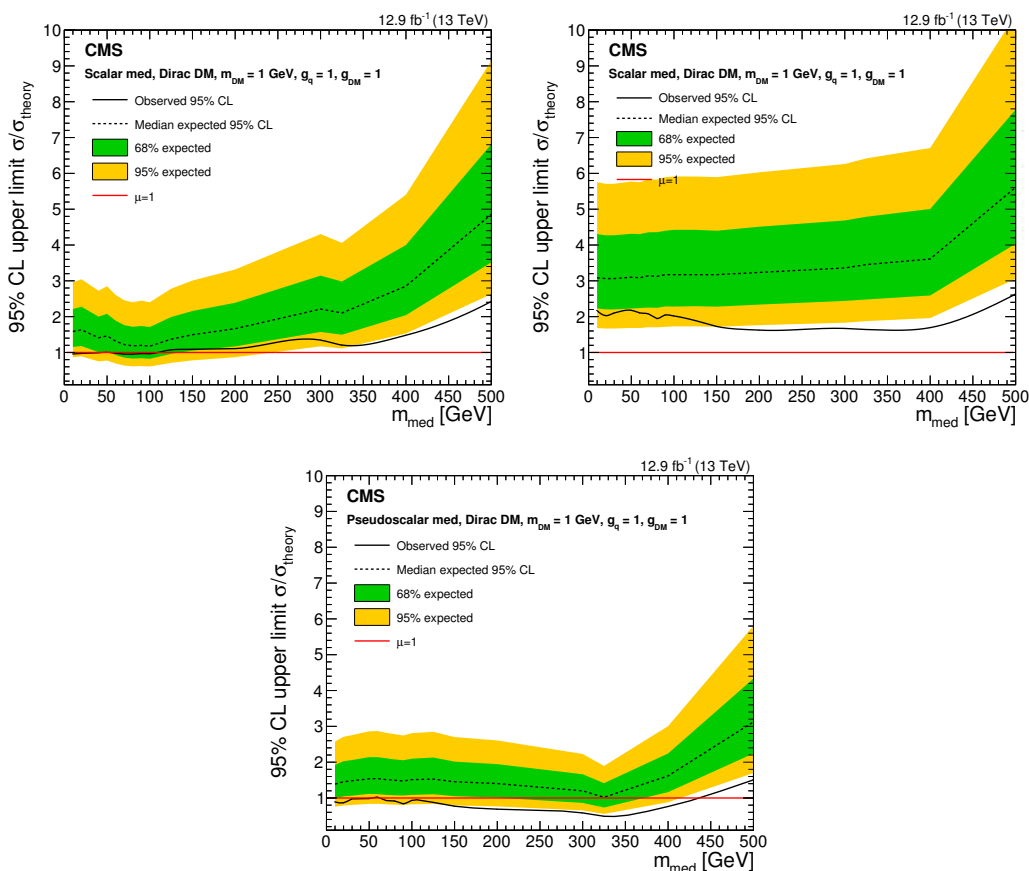
Figure 10. Expected (dotted black line) and observed (solid black line) 95% CL upper limits on the signal strength μ as a function of the mediator mass for the spin-0 models. The horizontal red line denotes $\mu = 1$. Limits for the scalar model on the combined cross section of the monojet and mono-V processes (upper left). Limits for the scalar (upper right) and pseudoscalar (bottom) models, respectively, assuming only the monojet signal process.

Category	Expected limit	Observed limit	±1 s.d.	Expected signal composition
Mono-V	0.72	1.17	[0.51–1.02]	39.6% ggH, 6.9% VBF, 32.4% WH, 21.1% ZH
Monojet	0.85	0.48	[0.58–1.27]	71.5% ggH, 20.3% VBF, 4.4% WH, 3.8% ZH
Combined	0.56	0.44	[0.40–0.81]	—

Table 5. Expected and observed 95% CL upper limits on the invisible branching fraction of the Higgs boson. Limits are tabulated for the monojet and mono-V categories separately, and for their combination. The one standard deviation uncertainty range on the expected limits is listed. The signal composition in terms of gluon fusion, vector boson fusion, and an associated production with a W or Z boson is also provided.
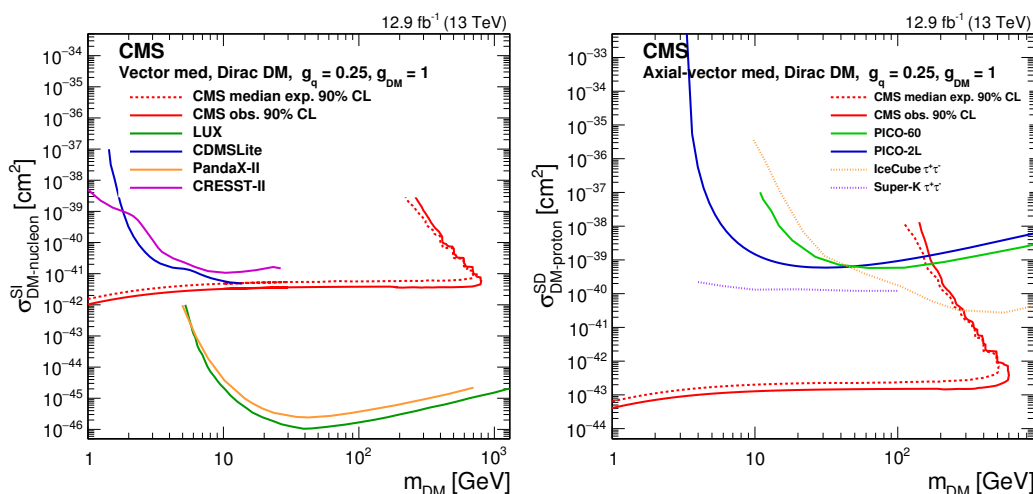
Figure 11. Exclusion limits at 90% CL in the m_{DM} vs. $\sigma_{\mathrm{SI/SD}}$ plane for vector (left) and axial-vector (right) mediator models. The solid (dotted) red line shows the contour for the observed (expected) exclusion in this search. Limits from the CDMSLite [91], LUX [92], PandaX-II [93], and CRESST-II [94] experiments are shown for the vector mediator. Limits from the PICO-2L [95], PICO-60 [96], IceCube [97], and Super-Kamiokande [98] experiments are shown for the axial-vector mediator.
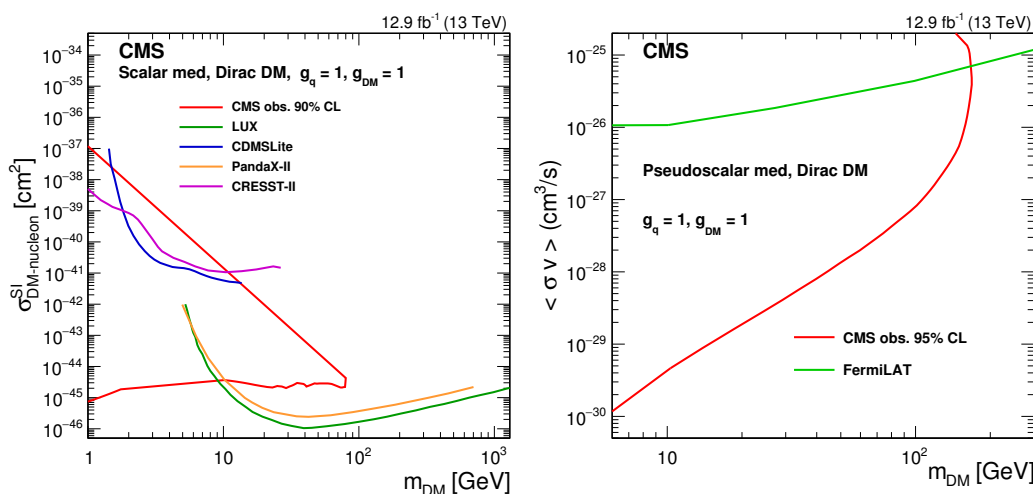
Figure 12. Exclusion limits at 90% CL in the m_{DM} vs. $\sigma_{\mathrm{SI/SD}}$ plane for the scalar mediator model (left). The observed exclusion in this search (red line) is compared to the results from the CDMSLite [91], LUX [92], PandaX-II [93], and CRESST-II [94] experiments. For the pseudoscalar mediator (right), limits at 95% CL are compared to the velocity-averaged DM annihilation cross section upper limits from Fermi-LAT [90]. There are no comparable limits from direct detection experiments as the scattering cross section between DM particles and SM quarks is suppressed at nonrelativistic velocities for a pseudoscalar mediator [99, 100].
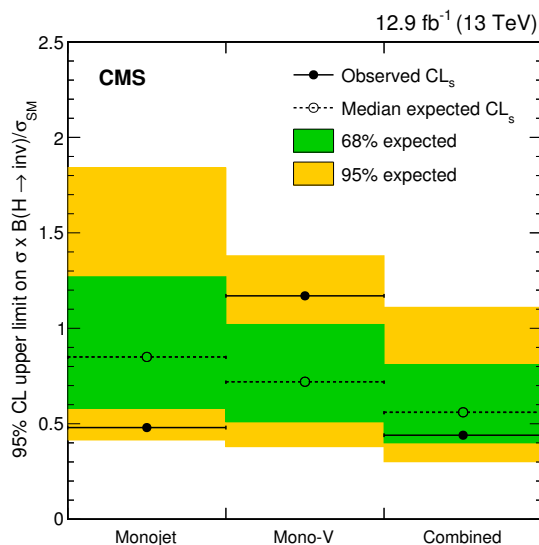
Figure 13. Expected (dotted black line) and observed (solid black line) 95% CL upper limits on the invisible branching fraction of a 125 GeV SM-like Higgs boson. Limits are shown for the monojet and mono-V categories separately, and also for their combination.

served with respect to the standard model backgrounds. Limits are computed on the DM production cross section using simplified models in which DM production is mediated by spin-1 or spin-0 particles. Vector and axial-vector mediators with masses up to 1.95 TeV are excluded at 95% confidence level, assuming a coupling strength of 0.25 between the mediators and the standard model fermions, and a coupling strength of 1.0 between the mediators and the DM particles. The results of this search provide the strongest constraints on DM pair production through vector and axial-vector mediators at a particle collider. Scalar and pseudoscalar mediators with masses up to 100 and 430 GeV, respectively, are excluded at 95% confidence level, assuming the coupling of the spin-0 mediators with DM particles to be 1.0 and the coupling of the spin-0 mediators with standard model fermions to be the same as the standard model Yukawa interactions. When compared to the direct detection experiments, the limits obtained from this search provide stronger constraints for dark matter masses less than 5, 9, and 550 GeV, assuming vector, scalar, and axial-vector mediators, respectively. The search yields stronger constraints for dark matter masses less than 200 GeV, assuming a pseudoscalar mediator, when compared to the indirect detection results from Fermi-LAT. The search also yields an observed (expected) 95% confidence level upper limit of 0.44 (0.56) on the invisible branching fraction of a standard model-like 125 GeV Higgs boson, assuming the standard model production cross section.

Acknowledgments

A   Supplementary material

Tables 3 and 4 provide the estimates of various background processes in the monojet and mono-V signal regions, respectively, that are obtained by performing a fit across all the control samples. The resulting correlations between the uncertainties in the estimated
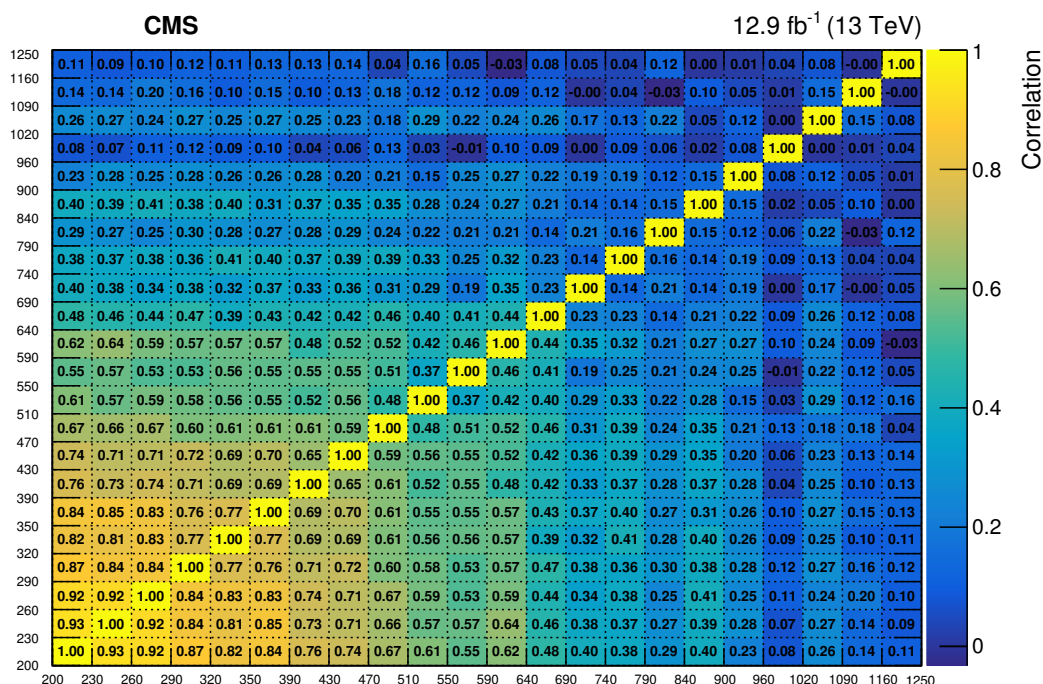
Figure 14. Correlations between the uncertainties in the estimated background yields in all the $E_{\mathrm{T}}^{\mathrm{miss}}$ bins of the monojet signal region. The boundaries of the $E_{\mathrm{T}}^{\mathrm{miss}}$ bins, expressed in GeV, are shown at the bottom and on the left.
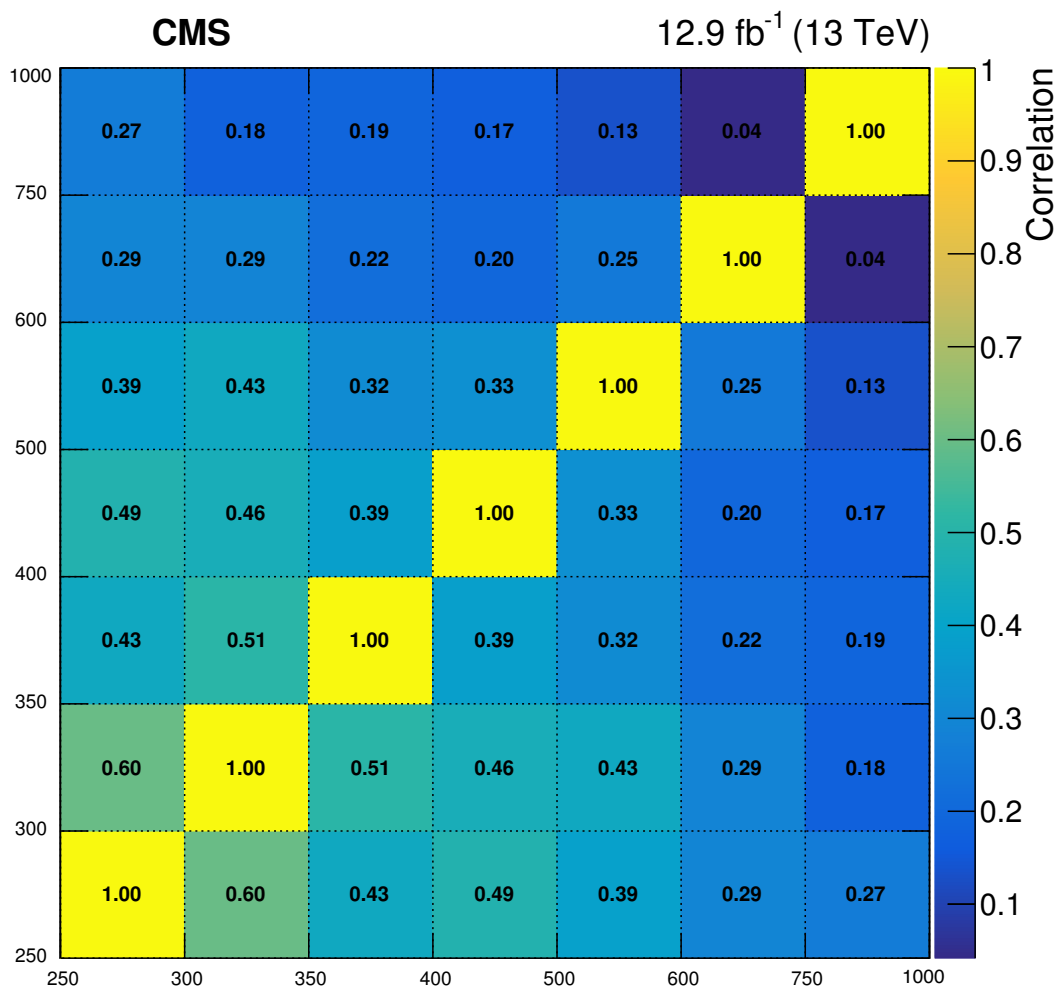
Figure 15. Correlations between the uncertainties in the estimated background yields in all the E_T^{miss} bins of the mono-V signal region. The boundaries of the E_T^{miss} bins, expressed in GeV, are shown at the bottom and on the left.

background yields across all the E_T^{miss} bins of the monojet and mono-V signal regions are shown in figure 14 and 15, respectively.

Open Access. This article is distributed under the terms of the Creative Commons Attribution License ([CC-BY 4.0](#)), which permits any use, distribution and reproduction in any medium, provided the original author(s) and source are credited.

References

[1] G. Bertone, D. Hooper and J. Silk, *Particle dark matter: evidence, candidates and constraints*, *Phys. Rept.* **405** (2005) 279 [hep-ph/0404175] [INSPIRE].

[2] J.L. Feng, *Dark matter candidates from particle physics and methods of detection*, *Ann. Rev. Astron. Astrophys.* **48** (2010) 495 [arXiv:1003.0904] [inSPIRE].

[3] T.A. Porter, R.P. Johnson and P.W. Graham, *Dark matter searches with astroparticle data*, *Ann. Rev. Astron. Astrophys.* **49** (2011) 155 [arXiv:1104.2836] [inSPIRE].

[4] M. Beltrán, D. Hooper, E.W. Kolb, Z.A.C. Krusberg and T.M.P. Tait, *Maverick dark matter at colliders*, *JHEP* **09** (2010) 037 [arXiv:1002.4137] [inSPIRE].

[5] J. Goodman, M. Ibe, A. Rajaraman, W. Shepherd, T.M.P. Tait and H.-B. Yu, *Constraints on dark matter from colliders*, *Phys. Rev.* **D 82** (2010) 116010 [arXiv:1008.1783] [inSPIRE].

[6] Y. Bai, P.J. Fox and R. Harnik, *The Tevatron at the frontier of dark matter direct detection*, *JHEP* **12** (2010) 048 [arXiv:1005.3797] [inSPIRE].

[7] N.F. Bell, J.B. Dent, A.J. Galea, T.D. Jacques, L.M. Krauss and T.J. Weiler, *Searching for dark matter at the LHC with a mono-Z*, *Phys. Rev.* **D 86** (2012) 096011 [arXiv:1209.0231] [inSPIRE].

[8] H. An, R. Huo and L.-T. Wang, *Searching for low mass dark portal at the LHC*, *Phys. Dark Univ.* **2** (2013) 50 [arXiv:1212.2221] [inSPIRE].

[9] L.M. Carpenter, A. Nelson, C. Shimmin, T.M.P. Tait and D. Whiteson, *Collider searches for dark matter in events with a Z boson and missing energy*, *Phys. Rev.* **D 87** (2013) 074005 [arXiv:1212.3352] [inSPIRE].

[10] ATLAS collaboration, *Observation of a new particle in the search for the Standard Model Higgs boson with the ATLAS detector at the LHC*, *Phys. Lett.* **B 716** (2012) 1 [arXiv:1207.7214] [inSPIRE].

[11] CMS collaboration, *Observation of a new boson at a mass of 125 GeV with the CMS experiment at the LHC*, *Phys. Lett.* **B 716** (2012) 30 [arXiv:1207.7235] [inSPIRE].

[12] CMS collaboration, *Observation of a new boson with mass near 125 GeV in pp collisions at $\sqrt{s} = 7$ and 8 TeV*, *JHEP* **06** (2013) 081 [arXiv:1303.4571] [inSPIRE].

[13] K.Y. Lee, Y.G. Kim and S. Shin, *Singlet fermionic dark matter as a natural Higgs portal model*, in *Proceedings, 16th International Conference on Supersymmetry and the Unification of Fundamental Interactions (SUSY08)*, Seoul Korea, (2008) [arXiv:0809.2745] [inSPIRE].

[14] S. Baek, P. Ko, W.-I. Park and E. Senaha, *Higgs portal vector dark matter: revisited*, *JHEP* **05** (2013) 036 [arXiv:1212.2131] [inSPIRE].

[15] A. Djouadi, O. Lebedev, Y. Mambrini and J. Quevillon, *Implications of LHC searches for Higgs-portal dark matter*, *Phys. Lett.* **B 709** (2012) 65 [arXiv:1112.3299] [inSPIRE].

[16] A. Djouadi, A. Falkowski, Y. Mambrini and J. Quevillon, *Direct detection of Higgs-portal dark matter at the LHC*, *Eur. Phys. J.* **C 73** (2013) 2455 [arXiv:1205.3169] [inSPIRE].

[17] A. Beniwal et al., *Combined analysis of effective Higgs portal dark matter models*, *Phys. Rev.* **D 93** (2016) 115016 [arXiv:1512.06458] [inSPIRE].

[18] ATLAS collaboration, *Search for dark matter in events with a hadronically decaying W or Z boson and missing transverse momentum in pp collisions at $\sqrt{s} = 8$ TeV with the ATLAS detector*, *Phys. Rev. Lett.* **112** (2014) 041802 [arXiv:1309.4017] [inSPIRE].

[19] CMS collaboration, *Search for dark matter, extra dimensions and unparticles in monojet events in proton-proton collisions at $\sqrt{s} = 8$ TeV*, *Eur. Phys. J.* **C 75** (2015) 235 [arXiv:1408.3583] [INSPIRE].

[20] ATLAS collaboration, *Search for new phenomena in final states with an energetic jet and large missing transverse momentum in pp collisions at $\sqrt{s} = 8$ TeV with the ATLAS detector*, *Eur. Phys. J.* **C 75** (2015) 299 [*Erratum ibid.* **C 75** (2015) 408] [arXiv:1502.01518] [INSPIRE].

[21] CMS collaboration, *Search for dark matter in proton-proton collisions at 8 TeV with missing transverse momentum and vector boson tagged jets*, *JHEP* **12** (2016) 083 [arXiv:1607.05764] [INSPIRE].

[22] ATLAS collaboration, *Search for new phenomena in final states with an energetic jet and large missing transverse momentum in pp collisions at $\sqrt{s} = 13$ TeV using the ATLAS detector*, *Phys. Rev.* **D 94** (2016) 032005 [arXiv:1604.07773] [INSPIRE].

[23] ATLAS collaboration, *Search for dark matter produced in association with a hadronically decaying vector boson in pp collisions at $\sqrt{s} = 13$ TeV with the ATLAS detector*, *Phys. Lett.* **B 763** (2016) 251 [arXiv:1608.02372] [INSPIRE].

[24] H. An, X. Ji and L.-T. Wang, *Light dark matter and Z' dark force at colliders*, *JHEP* **07** (2012) 182 [arXiv:1202.2894] [INSPIRE].

[25] O. Buchmueller, M.J. Dolan and C. McCabe, *Beyond effective field theory for dark matter searches at the LHC*, *JHEP* **01** (2014) 025 [arXiv:1308.6799] [INSPIRE].

[26] S.A. Malik et al., *Interplay and characterization of dark matter searches at colliders and in direct detection experiments*, *Phys. Dark Univ.* **9-10** (2015) 51 [arXiv:1409.4075] [INSPIRE].

[27] P. Harris, V.V. Khoze, M. Spannowsky and C. Williams, *Constraining dark sectors at colliders: beyond the effective theory approach*, *Phys. Rev.* **D 91** (2015) 055009 [arXiv:1411.0535] [INSPIRE].

[28] M.R. Buckley, D. Feld and D. Goncalves, *Scalar simplified models for dark matter*, *Phys. Rev.* **D 91** (2015) 015017 [arXiv:1410.6497] [INSPIRE].

[29] U. Haisch and E. Re, *Simplified dark matter top-quark interactions at the LHC*, *JHEP* **06** (2015) 078 [arXiv:1503.00691] [INSPIRE].

[30] P. Harris, V.V. Khoze, M. Spannowsky and C. Williams, *Closing up on dark sectors at colliders: from 14 to 100 TeV*, *Phys. Rev.* **D 93** (2016) 054030 [arXiv:1509.02904] [INSPIRE].

[31] ATLAS collaboration, *Search for invisible decays of a Higgs boson produced in association with a Z boson in ATLAS*, *Phys. Rev. Lett.* **112** (2014) 201802 [arXiv:1402.3244] [INSPIRE].

[32] CMS collaboration, *Search for invisible decays of Higgs bosons in the vector boson fusion and associated ZH production modes*, *Eur. Phys. J.* **C 74** (2014) 2980 [arXiv:1404.1344] [INSPIRE].

[33] ATLAS collaboration, *Search for invisible decays of the Higgs boson produced in association with a hadronically decaying vector boson in pp collisions at $\sqrt{s} = 8$ TeV with the ATLAS detector*, *Eur. Phys. J.* **C 75** (2015) 337 [arXiv:1504.04324] [INSPIRE].

[34] ATLAS collaboration, *Search for invisible decays of a Higgs boson using vector-boson fusion in pp collisions at $\sqrt{s} = 8\,TeV$ with the ATLAS detector*, *JHEP* **01** (2016) 172 [arXiv:1508.07869] [INSPIRE].

[35] ATLAS collaboration, *Constraints on new phenomena via Higgs boson couplings and invisible decays with the ATLAS detector*, *JHEP* **11** (2015) 206 [arXiv:1509.00672] [INSPIRE].

[36] CMS collaboration, *Searches for invisible decays of the Higgs boson in pp collisions at $\sqrt{s} = 7$, 8 and 13 TeV*, *JHEP* **02** (2017) 135 [arXiv:1610.09218] [INSPIRE].

[37] ATLAS and CMS collaborations, *Measurements of the Higgs boson production and decay rates and constraints on its couplings from a combined ATLAS and CMS analysis of the LHC pp collision data at $\sqrt{s} = 7$ and 8 TeV*, *JHEP* **08** (2016) 045 [arXiv:1606.02266] [INSPIRE].

[38] CMS collaboration, *The CMS experiment at the CERN LHC*, 2008 *JINST* **3** S08004 [INSPIRE].

[39] CMS collaboration, *Particle-flow event reconstruction in CMS and performance for jets, taus and MET*, CMS-PAS-PFT-09-001, CERN, Geneva Switzerland, (2009).

[40] CMS collaboration, *Commissioning of the particle-flow event reconstruction with the first LHC collisions recorded in the CMS detector*, CMS-PAS-PFT-10-001, CERN, Geneva Switzerland, (2010).

[41] M. Cacciari, G.P. Salam and G. Soyez, *The anti-k_t jet clustering algorithm*, *JHEP* **04** (2008) 063 [arXiv:0802.1189] [INSPIRE].

[42] CMS collaboration, *Determination of jet energy calibration and transverse momentum resolution in CMS*, 2011 *JINST* **6** P11002 [arXiv:1107.4277] [INSPIRE].

[43] CMS collaboration, *Performance of missing energy reconstruction in 13 TeV pp collision data using the CMS detector*, CMS-PAS-JME-16-004, CERN, Geneva Switzerland, (2016).

[44] J. Alwall et al., *The automated computation of tree-level and next-to-leading order differential cross sections and their matching to parton shower simulations*, *JHEP* **07** (2014) 079 [arXiv:1405.0301] [INSPIRE].

[45] P. Nason, *A new method for combining NLO QCD with shower Monte Carlo algorithms*, *JHEP* **11** (2004) 040 [hep-ph/0409146] [INSPIRE].

[46] S. Frixione, P. Nason and C. Oleari, *Matching NLO QCD computations with parton shower simulations: the POWHEG method*, *JHEP* **11** (2007) 070 [arXiv:0709.2092] [INSPIRE].

[47] S. Alioli, P. Nason, C. Oleari and E. Re, *A general framework for implementing NLO calculations in shower Monte Carlo programs: the POWHEG BOX*, *JHEP* **06** (2010) 043 [arXiv:1002.2581] [INSPIRE].

[48] T. Sjöstrand et al., *An introduction to PYTHIA* 8.2, *Comput. Phys. Commun.* **191** (2015) 159 [arXiv:1410.3012] [INSPIRE].

[49] U. Haisch, F. Kahlhoefer and E. Re, *QCD effects in mono-jet searches for dark matter*, *JHEP* **12** (2013) 007 [arXiv:1310.4491] [INSPIRE].

[50] Y. Gao, A.V. Gritsan, Z. Guo, K. Melnikov, M. Schulze and N.V. Tran, *Spin determination of single-produced resonances at hadron colliders*, *Phys. Rev.* **D 81** (2010) 075022 [arXiv:1001.3396] [INSPIRE].

[51] S. Bolognesi et al., *On the spin and parity of a single-produced resonance at the LHC*, *Phys. Rev.* **D 86** (2012) 095031 [arXiv:1208.4018] [InSPIRE].

[52] I. Anderson et al., *Constraining anomalous HVV interactions at proton and lepton colliders*, *Phys. Rev.* **D 89** (2014) 035007 [arXiv:1309.4819] [InSPIRE].

[53] CMS collaboration, *Event generator tunes obtained from underlying event and multiparton scattering measurements*, *Eur. Phys. J.* **C 76** (2016) 155 [arXiv:1512.00815] [InSPIRE].

[54] R. Frederix and S. Frixione, *Merging meets matching in MC@NLO*, *JHEP* **12** (2012) 061 [arXiv:1209.6215] [InSPIRE].

[55] M.L. Mangano, M. Moretti, F. Piccinini and M. Treccani, *Matching matrix elements and shower evolution for top-quark production in hadronic collisions*, *JHEP* **01** (2007) 013 [hep-ph/0611129] [InSPIRE].

[56] NNPDF collaboration, R.D. Ball et al., *Parton distributions for the LHC run II*, *JHEP* **04** (2015) 040 [arXiv:1410.8849] [InSPIRE].

[57] GEANT4 collaboration, S. Agostinelli et al., *GEANT4: a simulation toolkit*, *Nucl. Instrum. Meth.* **A 506** (2003) 250 [InSPIRE].

[58] CMS collaboration, *Performance of electron reconstruction and selection with the CMS detector in proton-proton collisions at $\sqrt{s} = 8\,TeV$*, 2015 *JINST* **10** P06005 [arXiv:1502.02701] [InSPIRE].

[59] CMS collaboration, *Reconstruction and identification of τ lepton decays to hadrons and ν_τ at CMS*, 2016 *JINST* **11** P01019 [arXiv:1510.07488] [InSPIRE].

[60] CMS collaboration, *Performance of photon reconstruction and identification with the CMS detector in proton-proton collisions at $\sqrt{s} = 8\,TeV$*, 2015 *JINST* **10** P08010 [arXiv:1502.02702] [InSPIRE].

[61] CMS collaboration, *Identification of b-quark jets with the CMS experiment*, 2013 *JINST* **8** P04013 [arXiv:1211.4462] [InSPIRE].

[62] CMS collaboration, *Identification of b-quark jets at the CMS experiment in the LHC run 2*, CMS-PAS-BTV-15-001, CERN, Geneva Switzerland, (2015).

[63] J. Thaler and K. Van Tilburg, *Identifying boosted objects with N-subjettiness*, *JHEP* **03** (2011) 015 [arXiv:1011.2268] [InSPIRE].

[64] S.D. Ellis, C.K. Vermilion and J.R. Walsh, *Recombination algorithms and jet substructure: pruning as a tool for heavy particle searches*, *Phys. Rev.* **D 81** (2010) 094023 [arXiv:0912.0033] [InSPIRE].

[65] Y.L. Dokshitzer, G.D. Leder, S. Moretti and B.R. Webber, *Better jet clustering algorithms*, *JHEP* **08** (1997) 001 [hep-ph/9707323] [InSPIRE].

[66] M. Wobisch and T. Wengler, *Hadronization corrections to jet cross-sections in deep inelastic scattering*, in *Monte Carlo generators for HERA physics. Proceedings, Workshop*, Hamburg Germany, (1998), pg. 270 [hep-ph/9907280] [InSPIRE].

[67] J.H. Kuhn, A. Kulesza, S. Pozzorini and M. Schulze, *Electroweak corrections to hadronic photon production at large transverse momenta*, *JHEP* **03** (2006) 059 [hep-ph/0508253] [InSPIRE].

[68] S. Kallweit, J.M. Lindert, P. Maierhöfer, S. Pozzorini and M. Schönherr, *NLO electroweak automation and precise predictions for W +multijet production at the LHC*, *JHEP* **04** (2015) 012 [arXiv:1412.5157] [INSPIRE].

[69] S. Kallweit, J.M. Lindert, P. Maierhofer, S. Pozzorini and M. Schönherr, *NLO QCD+EW predictions for V +jets including off-shell vector-boson decays and multijet merging*, *JHEP* **04** (2016) 021 [arXiv:1511.08692] [INSPIRE].

[70] CMS collaboration, *Search for new physics with jets and missing transverse momentum in pp collisions at $\sqrt{s} = 7\,TeV$*, *JHEP* **08** (2011) 155 [arXiv:1106.4503] [INSPIRE].

[71] M. Czakon, D. Heymes and A. Mitov, *High-precision differential predictions for top-quark pairs at the LHC*, *Phys. Rev. Lett.* **116** (2016) 082003 [arXiv:1511.00549] [INSPIRE].

[72] CMS collaboration, *Measurement of the top quark pair production cross section in proton-proton collisions at $\sqrt{s} = 13\,TeV$*, *Phys. Rev. Lett.* **116** (2016) 052002 [arXiv:1510.05302] [INSPIRE].

[73] CMS collaboration, *Measurement of the ZZ production cross section and $Z \to \ell^+\ell^-\ell'^+\ell'^-$ branching fraction in pp collisions at $\sqrt{s} = 13\,TeV$*, *Phys. Lett.* **B 763** (2016) 280 [arXiv:1607.08834] [INSPIRE].

[74] CMS collaboration, *Measurement of the WZ production cross section in pp collisions at $\sqrt{s} = 13\,TeV$*, *Phys. Lett.* **B 766** (2017) 268 [arXiv:1607.06943] [INSPIRE].

[75] CMS collaboration, *CMS luminosity measurement for the 2015 data-taking period*, CMS-PAS-LUM-15-001, CERN, Geneva Switzerland, (2015).

[76] CMS collaboration, *Performance of the CMS missing transverse momentum reconstruction in pp data at $\sqrt{s} = 8\,TeV$*, 2015 *JINST* **10** P02006 [arXiv:1411.0511] [INSPIRE].

[77] CMS collaboration, *Simplified likelihood for the re-interpretation of public CMS results*, CMS-NOTE-2017-001, CERN, Geneva Switzerland, (2017).

[78] D. Abercrombie et al., *Dark matter benchmark models for early LHC run-2 searches: report of the ATLAS/CMS dark matter forum*, arXiv:1507.00966 [INSPIRE].

[79] T. Junk, *Confidence level computation for combining searches with small statistics*, *Nucl. Instrum. Meth.* **A 434** (1999) 435 [hep-ex/9902006] [INSPIRE].

[80] A.L. Read, *Presentation of search results: the CL_s technique*, *J. Phys.* **G 28** (2002) 2693 [INSPIRE].

[81] G. Cowan, K. Cranmer, E. Gross and O. Vitells, *Asymptotic formulae for likelihood-based tests of new physics*, *Eur. Phys. J.* **C 71** (2011) 1554 [*Erratum ibid.* **C 73** (2013) 2501] [arXiv:1007.1727] [INSPIRE].

[82] J.F. Gunion, H.E. Haber and J. Wudka, *Sum rules for Higgs bosons*, *Phys. Rev.* **D 43** (1991) 904 [INSPIRE].

[83] PLANCK collaboration, P.A.R. Ade et al., *Planck 2015 results XIII. Cosmological parameters*, *Astron. Astrophys.* **594** (2016) A13 [arXiv:1502.01589] [INSPIRE].

[84] M. Backovic, K. Kong and M. McCaskey, *MadDM v.1.0: computation of dark matter relic abundance using MadGraph5*, *Physics of the Dark Universe* **5-6** (2014) 18 [arXiv:1308.4955] [INSPIRE].

[85] PLANCK collaboration, P.A.R. Ade et al., *Planck 2013 results XVI. Cosmological parameters*, *Astron. Astrophys.* **571** (2014) A16 [arXiv:1303.5076] [INSPIRE].

[86] T. du Pree, K. Hahn, P. Harris and C. Roskas, *Cosmological constraints on dark matter models for collider searches*, arXiv:1603.08525 [INSPIRE].

[87] M. Backović, M. Krämer, F. Maltoni, A. Martini, K. Mawatari and M. Pellen, *Higher-order QCD predictions for dark matter production at the LHC in simplified models with s-channel mediators*, *Eur. Phys. J.* **C 75** (2015) 482 [arXiv:1508.05327] [INSPIRE].

[88] O. Buchmueller, M.J. Dolan, S.A. Malik and C. McCabe, *Characterising dark matter searches at colliders and direct detection experiments: vector mediators*, *JHEP* **01** (2015) 037 [arXiv:1407.8257] [INSPIRE].

[89] G. Busoni et al., *Recommendations on presenting LHC searches for missing transverse energy signals using simplified s-channel models of dark matter*, arXiv:1603.04156 [INSPIRE].

[90] FERMI-LAT collaboration, M. Ackermann et al., *Searching for dark matter annihilation from milky way dwarf spheroidal galaxies with six years of Fermi Large Area Telescope data*, *Phys. Rev. Lett.* **115** (2015) 231301 [arXiv:1503.02641] [INSPIRE].

[91] SUPERCDMS collaboration, R. Agnese et al., *New results from the search for low-mass weakly interacting massive particles with the CDMS low ionization threshold experiment*, *Phys. Rev. Lett.* **116** (2016) 071301 [arXiv:1509.02448] [INSPIRE].

[92] LUX collaboration, D.S. Akerib et al., *Results from a search for dark matter in the complete LUX exposure*, *Phys. Rev. Lett.* **118** (2017) 021303 [arXiv:1608.07648] [INSPIRE].

[93] PANDAX-II collaboration, A. Tan et al., *Dark matter results from first 98.7 days of data from the PandaX-II experiment*, *Phys. Rev. Lett.* **117** (2016) 121303 [arXiv:1607.07400] [INSPIRE].

[94] CRESST collaboration, G. Angloher et al., *Results on light dark matter particles with a low-threshold CRESST-II detector*, *Eur. Phys. J.* **C 76** (2016) 25 [arXiv:1509.01515] [INSPIRE].

[95] PICO collaboration, C. Amole et al., *Improved dark matter search results from PICO-2L run 2*, *Phys. Rev.* **D 93** (2016) 061101 [arXiv:1601.03729] [INSPIRE].

[96] PICO collaboration, C. Amole et al., *Dark matter search results from the PICO-60 CF_3I bubble chamber*, *Phys. Rev.* **D 93** (2016) 052014 [arXiv:1510.07754] [INSPIRE].

[97] ICECUBE collaboration, M.G. Aartsen et al., *Improved limits on dark matter annihilation in the sun with the 79-string IceCube detector and implications for supersymmetry*, *JCAP* **04** (2016) 022 [arXiv:1601.00653] [INSPIRE].

[98] SUPER-KAMIOKANDE collaboration, K. Choi et al., *Search for neutrinos from annihilation of captured low-mass dark matter particles in the sun by Super-Kamiokande*, *Phys. Rev. Lett.* **114** (2015) 141301 [arXiv:1503.04858] [INSPIRE].

[99] U. Haisch, F. Kahlhoefer and J. Unwin, *The impact of heavy-quark loops on LHC dark matter searches*, *JHEP* **07** (2013) 125 [arXiv:1208.4605] [INSPIRE].

[100] A. Berlin, D. Hooper and S.D. McDermott, *Simplified dark matter models for the galactic center gamma-ray excess*, *Phys. Rev.* **D 89** (2014) 115022 [arXiv:1404.0022] [INSPIRE].

[101] LHC HIGGS CROSS SECTION WORKING GROUP collaboration, D. de Florian et al., *Handbook of LHC Higgs cross sections: 4. Deciphering the nature of the Higgs sector*, arXiv:1610.07922 [INSPIRE].

The CMS collaboration

Yerevan Physics Institute, Yerevan, Armenia

A.M. Sirunyan, A. Tumasyan

Institut für Hochenergiephysik, Wien, Austria

W. Adam, E. Asilar, T. Bergauer, J. Brandstetter, E. Brondolin, M. Dragicevic, J. Erö, M. Flechl, M. Friedl, R. Frühwirth[1], V.M. Ghete, C. Hartl, N. Hörmann, J. Hrubec, M. Jeitler[1], A. König, I. Krätschmer, D. Liko, T. Matsushita, I. Mikulec, D. Rabady, N. Rad, B. Rahbaran, H. Rohringer, J. Schieck[1], J. Strauss, W. Waltenberger, C.-E. Wulz[1]

Institute for Nuclear Problems, Minsk, Belarus

O. Dvornikov, V. Makarenko, V. Mossolov, J. Suarez Gonzalez, V. Zykunov

National Centre for Particle and High Energy Physics, Minsk, Belarus

N. Shumeiko

Universiteit Antwerpen, Antwerpen, Belgium

S. Alderweireldt, E.A. De Wolf, X. Janssen, J. Lauwers, M. Van De Klundert, H. Van Haevermaet, P. Van Mechelen, N. Van Remortel, A. Van Spilbeeck

Vrije Universiteit Brussel, Brussel, Belgium

S. Abu Zeid, F. Blekman, J. D'Hondt, N. Daci, I. De Bruyn, K. Deroover, S. Lowette, S. Moortgat, L. Moreels, A. Olbrechts, Q. Python, K. Skovpen, S. Tavernier, W. Van Doninck, P. Van Mulders, I. Van Parijs

Université Libre de Bruxelles, Bruxelles, Belgium

H. Brun, B. Clerbaux, G. De Lentdecker, H. Delannoy, G. Fasanella, L. Favart, R. Goldouzian, A. Grebenyuk, G. Karapostoli, T. Lenzi, A. Léonard, J. Luetic, T. Maerschalk, A. Marinov, A. Randle-conde, T. Seva, C. Vander Velde, P. Vanlaer, D. Vannerom, R. Yonamine, F. Zenoni, F. Zhang[2]

Ghent University, Ghent, Belgium

T. Cornelis, D. Dobur, A. Fagot, M. Gul, I. Khvastunov, D. Poyraz, S. Salva, R. Schöfbeck, M. Tytgat, W. Van Driessche, E. Yazgan, N. Zaganidis

Université Catholique de Louvain, Louvain-la-Neuve, Belgium

H. Bakhshiansohi, C. Beluffi[3], O. Bondu, S. Brochet, G. Bruno, A. Caudron, S. De Visscher, C. Delaere, M. Delcourt, B. Francois, A. Giammanco, A. Jafari, M. Komm, G. Krintiras, V. Lemaitre, A. Magitteri, A. Mertens, M. Musich, K. Piotrzkowski, L. Quertenmont, M. Selvaggi, M. Vidal Marono, S. Wertz

Université de Mons, Mons, Belgium

N. Beliy

Centro Brasileiro de Pesquisas Fisicas, Rio de Janeiro, Brazil

W.L. Aldá Júnior, F.L. Alves, G.A. Alves, L. Brito, C. Hensel, A. Moraes, M.E. Pol, P. Rebello Teles

Universidade do Estado do Rio de Janeiro, Rio de Janeiro, Brazil

E. Belchior Batista Das Chagas, W. Carvalho, J. Chinellato[4], A. Custódio, E.M. Da Costa, G.G. Da Silveira[5], D. De Jesus Damiao, C. De Oliveira Martins, S. Fonseca De Souza, L.M. Huertas Guativa, H. Malbouisson, D. Matos Figueiredo, C. Mora Herrera, L. Mundim, H. Nogima, W.L. Prado Da Silva, A. Santoro, A. Sznajder, E.J. Tonelli Manganote[4], F. Torres Da Silva De Araujo, A. Vilela Pereira

Universidade Estadual Paulista [a], Universidade Federal do ABC [b], São Paulo, Brazil

S. Ahuja[a], C.A. Bernardes[a], S. Dogra[a], T.R. Fernandez Perez Tomei[a], E.M. Gregores[b], P.G. Mercadante[b], C.S. Moon[a], S.F. Novaes[a], Sandra S. Padula[a], D. Romero Abad[b], J.C. Ruiz Vargas[a]

Institute for Nuclear Research and Nuclear Energy, Sofia, Bulgaria

A. Aleksandrov, R. Hadjiiska, P. Iaydjiev, M. Rodozov, S. Stoykova, G. Sultanov, M. Vutova

University of Sofia, Sofia, Bulgaria

A. Dimitrov, I. Glushkov, L. Litov, B. Pavlov, P. Petkov

Beihang University, Beijing, China

W. Fang[6]

Institute of High Energy Physics, Beijing, China

M. Ahmad, J.G. Bian, G.M. Chen, H.S. Chen, M. Chen, Y. Chen[7], T. Cheng, C.H. Jiang, D. Leggat, Z. Liu, F. Romeo, M. Ruan, S.M. Shaheen, A. Spiezia, J. Tao, C. Wang, Z. Wang, H. Zhang, J. Zhao

State Key Laboratory of Nuclear Physics and Technology, Peking University, Beijing, China

Y. Ban, G. Chen, Q. Li, S. Liu, Y. Mao, S.J. Qian, D. Wang, Z. Xu

Universidad de Los Andes, Bogota, Colombia

C. Avila, A. Cabrera, L.F. Chaparro Sierra, C. Florez, J.P. Gomez, C.F. González Hernández, J.D. Ruiz Alvarez[8], J.C. Sanabria

University of Split, Faculty of Electrical Engineering, Mechanical Engineering and Naval Architecture, Split, Croatia

N. Godinovic, D. Lelas, I. Puljak, P.M. Ribeiro Cipriano, T. Sculac

University of Split, Faculty of Science, Split, Croatia

Z. Antunovic, M. Kovac

Institute Rudjer Boskovic, Zagreb, Croatia

V. Brigljevic, D. Ferencek, K. Kadija, B. Mesic, T. Susa

University of Cyprus, Nicosia, Cyprus

M.W. Ather, A. Attikis, G. Mavromanolakis, J. Mousa, C. Nicolaou, F. Ptochos, P.A. Razis, H. Rykaczewski

Charles University, Prague, Czech Republic

M. Finger[9], M. Finger Jr.[9]

Universidad San Francisco de Quito, Quito, Ecuador

E. Carrera Jarrin

Academy of Scientific Research and Technology of the Arab Republic of Egypt, Egyptian Network of High Energy Physics, Cairo, Egypt

A.A. Abdelalim[10,11], S. Khalil[11], E. Salama[12,13]

National Institute of Chemical Physics and Biophysics, Tallinn, Estonia

M. Kadastik, L. Perrini, M. Raidal, A. Tiko, C. Veelken

Department of Physics, University of Helsinki, Helsinki, Finland

P. Eerola, J. Pekkanen, M. Voutilainen

Helsinki Institute of Physics, Helsinki, Finland

J. Härkönen, T. Järvinen, V. Karimäki, R. Kinnunen, T. Lampén, K. Lassila-Perini, S. Lehti, T. Lindén, P. Luukka, J. Tuominiemi, E. Tuovinen, L. Wendland

Lappeenranta University of Technology, Lappeenranta, Finland

J. Talvitie, T. Tuuva

IRFU, CEA, Université Paris-Saclay, Gif-sur-Yvette, France

M. Besancon, F. Couderc, M. Dejardin, D. Denegri, B. Fabbro, J.L. Faure, C. Favaro, F. Ferri, S. Ganjour, S. Ghosh, A. Givernaud, P. Gras, G. Hamel de Monchenault, P. Jarry, I. Kucher, E. Locci, M. Machet, J. Malcles, J. Rander, A. Rosowsky, M. Titov

Laboratoire Leprince-Ringuet, Ecole Polytechnique, IN2P3-CNRS, Palaiseau, France

A. Abdulsalam, I. Antropov, S. Baffioni, F. Beaudette, P. Busson, L. Cadamuro, E. Chapon, C. Charlot, O. Davignon, R. Granier de Cassagnac, M. Jo, S. Lisniak, P. Miné, M. Nguyen, C. Ochando, G. Ortona, P. Paganini, P. Pigard, S. Regnard, R. Salerno, Y. Sirois, A.G. Stahl Leiton, T. Strebler, Y. Yilmaz, A. Zabi, A. Zghiche

Institut Pluridisciplinaire Hubert Curien (IPHC), Université de Strasbourg, CNRS-IN2P3

J.-L. Agram[14], J. Andrea, D. Bloch, J.-M. Brom, M. Buttignol, E.C. Chabert, N. Chanon, C. Collard, E. Conte[14], X. Coubez, J.-C. Fontaine[14], D. Gelé, U. Goerlach, A.-C. Le Bihan, P. Van Hove

Centre de Calcul de l'Institut National de Physique Nucleaire et de Physique des Particules, CNRS/IN2P3, Villeurbanne, France

S. Gadrat

Université de Lyon, Université Claude Bernard Lyon 1, CNRS-IN2P3, Institut de Physique Nucléaire de Lyon, Villeurbanne, France

S. Beauceron, C. Bernet, G. Boudoul, C.A. Carrillo Montoya, R. Chierici, D. Contardo, B. Courbon, P. Depasse, H. El Mamouni, J. Fay, S. Gascon, M. Gouzevitch, G. Grenier,

B. Ille, F. Lagarde, I.B. Laktineh, M. Lethuillier, L. Mirabito, A.L. Pequegnot, S. Perries, A. Popov[15], V. Sordini, M. Vander Donckt, P. Verdier, S. Viret

Georgian Technical University, Tbilisi, Georgia
A. Khvedelidze[9]

Tbilisi State University, Tbilisi, Georgia
Z. Tsamalaidze[9]

RWTH Aachen University, I. Physikalisches Institut, Aachen, Germany
C. Autermann, S. Beranek, L. Feld, M.K. Kiesel, K. Klein, M. Lipinski, M. Preuten, C. Schomakers, J. Schulz, T. Verlage

RWTH Aachen University, III. Physikalisches Institut A, Aachen, Germany
A. Albert, M. Brodski, E. Dietz-Laursonn, D. Duchardt, M. Endres, M. Erdmann, S. Erdweg, T. Esch, R. Fischer, A. Güth, M. Hamer, T. Hebbeker, C. Heidemann, K. Hoepfner, S. Knutzen, M. Merschmeyer, A. Meyer, P. Millet, S. Mukherjee, M. Olschewski, K. Padeken, T. Pook, M. Radziej, H. Reithler, M. Rieger, F. Scheuch, L. Sonnenschein, D. Teyssier, S. Thüer

RWTH Aachen University, III. Physikalisches Institut B, Aachen, Germany
V. Cherepanov, G. Flügge, B. Kargoll, T. Kress, A. Künsken, J. Lingemann, T. Müller, A. Nehrkorn, A. Nowack, C. Pistone, O. Pooth, A. Stahl[16]

Deutsches Elektronen-Synchrotron, Hamburg, Germany
M. Aldaya Martin, T. Arndt, C. Asawatangtrakuldee, K. Beernaert, O. Behnke, U. Behrens, A.A. Bin Anuar, K. Borras[17], A. Campbell, P. Connor, C. Contreras-Campana, F. Costanza, C. Diez Pardos, G. Dolinska, G. Eckerlin, D. Eckstein, T. Eichhorn, E. Eren, E. Gallo[18], J. Garay Garcia, A. Geiser, A. Gizhko, J.M. Grados Luyando, A. Grohsjean, P. Gunnellini, A. Harb, J. Hauk, M. Hempel[19], H. Jung, A. Kalogeropoulos, O. Karacheban[19], M. Kasemann, J. Keaveney, C. Kleinwort, I. Korol, D. Krücker, W. Lange, A. Lelek, T. Lenz, J. Leonard, K. Lipka, A. Lobanov, W. Lohmann[19], R. Mankel, I.-A. Melzer-Pellmann, A.B. Meyer, G. Mittag, J. Mnich, A. Mussgiller, D. Pitzl, R. Placakyte, A. Raspereza, B. Roland, M.Ö. Sahin, P. Saxena, T. Schoerner-Sadenius, S. Spannagel, N. Stefaniuk, G.P. Van Onsem, R. Walsh, C. Wissing

University of Hamburg, Hamburg, Germany
V. Blobel, M. Centis Vignali, A.R. Draeger, T. Dreyer, E. Garutti, D. Gonzalez, J. Haller, M. Hoffmann, A. Junkes, R. Klanner, R. Kogler, N. Kovalchuk, T. Lapsien, I. Marchesini, D. Marconi, M. Meyer, M. Niedziela, D. Nowatschin, F. Pantaleo[16], T. Peiffer, A. Perieanu, C. Scharf, P. Schleper, A. Schmidt, S. Schumann, J. Schwandt, H. Stadie, G. Steinbrück, F.M. Stober, M. Stöver, H. Tholen, D. Troendle, E. Usai, L. Vanelderen, A. Vanhoefer, B. Vormwald

Institut für Experimentelle Kernphysik, Karlsruhe, Germany
M. Akbiyik, C. Barth, S. Baur, C. Baus, J. Berger, E. Butz, R. Caspart, T. Chwalek, F. Colombo, W. De Boer, A. Dierlamm, S. Fink, B. Freund, R. Friese, M. Giffels, A. Gilbert,

P. Goldenzweig, D. Haitz, F. Hartmann[16], S.M. Heindl, U. Husemann, F. Kassel[16], I. Katkov[15], S. Kudella, H. Mildner, M.U. Mozer, Th. Müller, M. Plagge, G. Quast, K. Rabbertz, S. Röcker, F. Roscher, M. Schröder, I. Shvetsov, G. Sieber, H.J. Simonis, R. Ulrich, S. Wayand, M. Weber, T. Weiler, S. Williamson, C. Wöhrmann, R. Wolf

Institute of Nuclear and Particle Physics (INPP), NCSR Demokritos, Aghia Paraskevi, Greece

G. Anagnostou, G. Daskalakis, T. Geralis, V.A. Giakoumopoulou, A. Kyriakis, D. Loukas, I. Topsis-Giotis

National and Kapodistrian University of Athens, Athens, Greece

S. Kesisoglou, A. Panagiotou, N. Saoulidou, E. Tziaferi

University of Ioánnina, Ioánnina, Greece

I. Evangelou, G. Flouris, C. Foudas, P. Kokkas, N. Loukas, N. Manthos, I. Papadopoulos, E. Paradas

MTA-ELTE Lendület CMS Particle and Nuclear Physics Group, Eötvös Loránd University, Budapest, Hungary

N. Filipovic, G. Pasztor

Wigner Research Centre for Physics, Budapest, Hungary

G. Bencze, C. Hajdu, D. Horvath[20], F. Sikler, V. Veszpremi, G. Vesztergombi[21], A.J. Zsigmond

Institute of Nuclear Research ATOMKI, Debrecen, Hungary

N. Beni, S. Czellar, J. Karancsi[22], A. Makovec, J. Molnar, Z. Szillasi

Institute of Physics, University of Debrecen

M. Bartók[21], P. Raics, Z.L. Trocsanyi, B. Ujvari

Indian Institute of Science (IISc)

J.R. Komaragiri

National Institute of Science Education and Research, Bhubaneswar, India

S. Bahinipati[23], S. Bhowmik[24], S. Choudhury[25], P. Mal, K. Mandal, A. Nayak[26], D.K. Sahoo[23], N. Sahoo, S.K. Swain

Panjab University, Chandigarh, India

S. Bansal, S.B. Beri, V. Bhatnagar, R. Chawla, U.Bhawandeep, A.K. Kalsi, A. Kaur, M. Kaur, R. Kumar, P. Kumari, A. Mehta, M. Mittal, J.B. Singh, G. Walia

University of Delhi, Delhi, India

Ashok Kumar, A. Bhardwaj, B.C. Choudhary, R.B. Garg, S. Keshri, S. Malhotra, M. Naimuddin, K. Ranjan, R. Sharma, V. Sharma

Saha Institute of Nuclear Physics, Kolkata, India

R. Bhattacharya, S. Bhattacharya, K. Chatterjee, S. Dey, S. Dutt, S. Dutta, S. Ghosh, N. Majumdar, A. Modak, K. Mondal, S. Mukhopadhyay, S. Nandan, A. Purohit, A. Roy, D. Roy, S. Roy Chowdhury, S. Sarkar, M. Sharan, S. Thakur

Indian Institute of Technology Madras, Madras, India

P.K. Behera

Bhabha Atomic Research Centre, Mumbai, India

R. Chudasama, D. Dutta, V. Jha, V. Kumar, A.K. Mohanty[16], P.K. Netrakanti, L.M. Pant,
P. Shukla, A. Topkar

Tata Institute of Fundamental Research-A, Mumbai, India

T. Aziz, S. Dugad, G. Kole, B. Mahakud, S. Mitra, G.B. Mohanty, B. Parida, N. Sur,
B. Sutar

Tata Institute of Fundamental Research-B, Mumbai, India

S. Banerjee, R.K. Dewanjee, S. Ganguly, M. Guchait, Sa. Jain, S. Kumar, M. Maity[24],
G. Majumder, K. Mazumdar, T. Sarkar[24], N. Wickramage[27]

Indian Institute of Science Education and Research (IISER), Pune, India

S. Chauhan, S. Dube, V. Hegde, A. Kapoor, K. Kothekar, S. Pandey, A. Rane, S. Sharma

Institute for Research in Fundamental Sciences (IPM), Tehran, Iran

S. Chenarani[28], E. Eskandari Tadavani, S.M. Etesami[28], M. Khakzad, M. Mohammadi
Najafabadi, M. Naseri, S. Paktinat Mehdiabadi[29], F. Rezaei Hosseinabadi, B. Safarzadeh[30],
M. Zeinali

University College Dublin, Dublin, Ireland

M. Felcini, M. Grunewald

INFN Sezione di Bari [a], **Università di Bari** [b], **Politecnico di Bari** [c], **Bari, Italy**

M. Abbrescia[a,b], C. Calabria[a,b], C. Caputo[a,b], A. Colaleo[a], D. Creanza[a,c], L. Cristella[a,b],
N. De Filippis[a,c], M. De Palma[a,b], L. Fiore[a], G. Iaselli[a,c], G. Maggi[a,c], M. Maggi[a],
G. Miniello[a,b], S. My[a,b], S. Nuzzo[a,b], A. Pompili[a,b], G. Pugliese[a,c], R. Radogna[a,b],
A. Ranieri[a], G. Selvaggi[a,b], A. Sharma[a], L. Silvestris[a,16], R. Venditti[a,b], P. Verwilligen[a]

INFN Sezione di Bologna [a], **Università di Bologna** [b], **Bologna, Italy**

G. Abbiendi[a], C. Battilana, D. Bonacorsi[a,b], S. Braibant-Giacomelli[a,b], L. Brigliadori[a,b],
R. Campanini[a,b], P. Capiluppi[a,b], A. Castro[a,b], F.R. Cavallo[a], S.S. Chhibra[a,b],
G. Codispoti[a,b], M. Cuffiani[a,b], G.M. Dallavalle[a], F. Fabbri[a], A. Fanfani[a,b], D. Fasanella[a,b],
P. Giacomelli[a], C. Grandi[a], L. Guiducci[a,b], S. Marcellini[a], G. Masetti[a], A. Montanari[a],
F.L. Navarria[a,b], A. Perrotta[a], A.M. Rossi[a,b], T. Rovelli[a,b], G.P. Siroli[a,b], N. Tosi[a,b,16]

INFN Sezione di Catania [a], **Università di Catania** [b], **Catania, Italy**

S. Albergo[a,b], S. Costa[a,b], A. Di Mattia[a], F. Giordano[a,b], R. Potenza[a,b], A. Tricomi[a,b],
C. Tuve[a,b]

INFN Sezione di Firenze [a], **Università di Firenze** [b], **Firenze, Italy**

G. Barbagli[a], V. Ciulli[a,b], C. Civinini[a], R. D'Alessandro[a,b], E. Focardi[a,b], P. Lenzi[a,b],
M. Meschini[a], S. Paoletti[a], L. Russo[a,31], G. Sguazzoni[a], D. Strom[a], L. Viliani[a,b,16]

INFN Laboratori Nazionali di Frascati, Frascati, Italy

L. Benussi, S. Bianco, F. Fabbri, D. Piccolo, F. Primavera[16]

INFN Sezione di Genova *a*, **Università di Genova** *b*, **Genova, Italy**

V. Calvelli*a,b*, F. Ferro*a*, M.R. Monge*a,b*, E. Robutti*a*, S. Tosi*a,b*

INFN Sezione di Milano-Bicocca *a*, **Università di Milano-Bicocca** *b*, **Milano, Italy**

L. Brianza*a,b,16*, F. Brivio*a,b*, V. Ciriolo, M.E. Dinardo*a,b*, S. Fiorendi*a,b,16*, S. Gennai*a*, A. Ghezzi*a,b*, P. Govoni*a,b*, M. Malberti*a,b*, S. Malvezzi*a*, R.A. Manzoni*a,b*, D. Menasce*a*, L. Moroni*a*, M. Paganoni*a,b*, D. Pedrini*a*, S. Pigazzini*a,b*, S. Ragazzi*a,b*, T. Tabarelli de Fatis*a,b*

INFN Sezione di Napoli *a*, **Università di Napoli 'Federico II'** *b*, **Napoli, Italy,** **Università della Basilicata** *c*, **Potenza, Italy, Università G. Marconi** *d*, **Roma, Italy**

S. Buontempo*a*, N. Cavallo*a,c*, G. De Nardo, S. Di Guida*a,d,16*, M. Esposito*a,b*, F. Fabozzi*a,c*, F. Fienga*a,b*, A.O.M. Iorio*a,b*, G. Lanza*a*, L. Lista*a*, S. Meola*a,d,16*, P. Paolucci*a,16*, C. Sciacca*a,b*, F. Thyssen*a*

INFN Sezione di Padova *a*, **Università di Padova** *b*, **Padova, Italy, Università di Trento** *c*, **Trento, Italy**

P. Azzi*a,16*, N. Bacchetta*a*, L. Benato*a,b*, D. Bisello*a,b*, A. Boletti*a,b*, R. Carlin*a,b*, A. Carvalho Antunes De Oliveira*a,b*, P. Checchia*a*, M. Dall'Osso*a,b*, P. De Castro Manzano*a*, T. Dorigo*a*, U. Dosselli*a*, F. Gasparini*a,b*, U. Gasparini*a,b*, A. Gozzelino*a*, S. Lacaprara*a*, M. Margoni*a,b*, A.T. Meneguzzo*a,b*, J. Pazzini*a,b*, N. Pozzobon*a,b*, P. Ronchese*a,b*, F. Simonetto*a,b*, E. Torassa*a*, M. Zanetti*a,b*, P. Zotto*a,b*, G. Zumerle*a,b*

INFN Sezione di Pavia *a*, **Università di Pavia** *b*, **Pavia, Italy**

A. Braghieri*a*, F. Fallavollita*a,b*, A. Magnani*a,b*, P. Montagna*a,b*, S.P. Ratti*a,b*, V. Re*a*, C. Riccardi*a,b*, P. Salvini*a*, I. Vai*a,b*, P. Vitulo*a,b*

INFN Sezione di Perugia *a*, **Università di Perugia** *b*, **Perugia, Italy**

L. Alunni Solestizi*a,b*, G.M. Bilei*a*, D. Ciangottini*a,b*, L. Fanò*a,b*, P. Lariccia*a,b*, R. Leonardi*a,b*, G. Mantovani*a,b*, V. Mariani*a,b*, M. Menichelli*a*, A. Saha*a*, A. Santocchia*a,b*

INFN Sezione di Pisa *a*, **Università di Pisa** *b*, **Scuola Normale Superiore di Pisa** *c*, **Pisa, Italy**

K. Androsov*a,31*, P. Azzurri*a,16*, G. Bagliesi*a*, J. Bernardini*a*, T. Boccali*a*, R. Castaldi*a*, M.A. Ciocci*a,31*, R. Dell'Orso*a*, S. Donato*a,c*, G. Fedi, A. Giassi*a*, M.T. Grippo*a,31*, F. Ligabue*a,c*, T. Lomtadze*a*, L. Martini*a,b*, A. Messineo*a,b*, F. Palla*a*, A. Rizzi*a,b*, A. Savoy-Navarro*a,32*, P. Spagnolo*a*, R. Tenchini*a*, G. Tonelli*a,b*, A. Venturi*a*, P.G. Verdini*a*

INFN Sezione di Roma *a*, **Università di Roma** *b*, **Roma, Italy**

L. Barone*a,b*, F. Cavallari*a*, M. Cipriani*a,b*, D. Del Re*a,b,16*, M. Diemoz*a*, S. Gelli*a,b*, E. Longo*a,b*, F. Margaroli*a,b*, B. Marzocchi*a,b*, P. Meridiani*a*, G. Organtini*a,b*, R. Paramatti*a,b*, F. Preiato*a,b*, S. Rahatlou*a,b*, C. Rovelli*a*, F. Santanastasio*a,b*

INFN Sezione di Torino ^{a}**, Università di Torino** ^{b}**, Torino, Italy, Università del Piemonte Orientale** ^{c}**, Novara, Italy**

N. Amapane^{a,b}, R. Arcidiacono^{a,c,16}, S. Argiro^{a,b}, M. Arneodo^{a,c}, N. Bartosik^a, R. Bellan^{a,b}, C. Biino^a, N. Cartiglia^a, F. Cenna^{a,b}, M. Costa^{a,b}, R. Covarelli^{a,b}, A. Degano^{a,b}, N. Demaria^a, L. Finco^{a,b}, B. Kiani^{a,b}, C. Mariotti^a, S. Maselli^a, E. Migliore^{a,b}, V. Monaco^{a,b}, E. Monteil^{a,b}, M. Monteno^a, M.M. Obertino^{a,b}, L. Pacher^{a,b}, N. Pastrone^a, M. Pelliccioni^a, G.L. Pinna Angioni^{a,b}, F. Ravera^{a,b}, A. Romero^{a,b}, M. Ruspa^{a,c}, R. Sacchi^{a,b}, K. Shchelina^{a,b}, V. Sola^a, A. Solano^{a,b}, A. Staiano^a, P. Traczyk^{a,b}

INFN Sezione di Trieste ^{a}**, Università di Trieste** ^{b}**, Trieste, Italy**

S. Belforte^a, M. Casarsa^a, F. Cossutti^a, G. Della Ricca^{a,b}, A. Zanetti^a

Kyungpook National University, Daegu, Korea

D.H. Kim, G.N. Kim, M.S. Kim, S. Lee, S.W. Lee, Y.D. Oh, S. Sekmen, D.C. Son, Y.C. Yang

Chonbuk National University, Jeonju, Korea

A. Lee

Chonnam National University, Institute for Universe and Elementary Particles, Kwangju, Korea

H. Kim

Hanyang University, Seoul, Korea

J.A. Brochero Cifuentes, T.J. Kim

Korea University, Seoul, Korea

S. Cho, S. Choi, Y. Go, D. Gyun, S. Ha, B. Hong, Y. Jo, Y. Kim, K. Lee, K.S. Lee, S. Lee, J. Lim, S.K. Park, Y. Roh

Seoul National University, Seoul, Korea

J. Almond, J. Kim, H. Lee, S.B. Oh, B.C. Radburn-Smith, S.h. Seo, U.K. Yang, H.D. Yoo, G.B. Yu

University of Seoul, Seoul, Korea

M. Choi, H. Kim, J.H. Kim, J.S.H. Lee, I.C. Park, G. Ryu, M.S. Ryu

Sungkyunkwan University, Suwon, Korea

Y. Choi, J. Goh, C. Hwang, J. Lee, I. Yu

Vilnius University, Vilnius, Lithuania

V. Dudenas, A. Juodagalvis, J. Vaitkus

National Centre for Particle Physics, Universiti Malaya, Kuala Lumpur, Malaysia

I. Ahmed, Z.A. Ibrahim, M.A.B. Md Ali^{33}, F. Mohamad Idris^{34}, W.A.T. Wan Abdullah, M.N. Yusli, Z. Zolkapli

Centro de Investigacion y de Estudios Avanzados del IPN, Mexico City, Mexico

H. Castilla-Valdez, E. De La Cruz-Burelo, I. Heredia-De La Cruz[35], A. Hernandez-Almada, R. Lopez-Fernandez, R. Magaña Villalba, J. Mejia Guisao, A. Sanchez-Hernandez

Universidad Iberoamericana, Mexico City, Mexico

S. Carrillo Moreno, C. Oropeza Barrera, F. Vazquez Valencia

Benemerita Universidad Autonoma de Puebla, Puebla, Mexico

S. Carpinteyro, I. Pedraza, H.A. Salazar Ibarguen, C. Uribe Estrada

Universidad Autónoma de San Luis Potosí, San Luis Potosí, Mexico

A. Morelos Pineda

University of Auckland, Auckland, New Zealand

D. Krofcheck

University of Canterbury, Christchurch, New Zealand

P.H. Butler

National Centre for Physics, Quaid-I-Azam University, Islamabad, Pakistan

A. Ahmad, Q. Hassan, H.R. Hoorani, W.A. Khan, S. Qazi, A. Saddique, M.A. Shah, M. Shoaib, M. Waqas

National Centre for Nuclear Research, Swierk, Poland

H. Bialkowska, M. Bluj, B. Boimska, T. Frueboes, M. Górski, M. Kazana, K. Nawrocki, K. Romanowska-Rybinska, M. Szleper, P. Zalewski

Institute of Experimental Physics, Faculty of Physics, University of Warsaw, Warsaw, Poland

K. Bunkowski, A. Byszuk[36], K. Doroba, A. Kalinowski, M. Konecki, J. Krolikowski, M. Misiura, M. Olszewski, M. Walczak

Laboratório de Instrumentação e Física Experimental de Partículas, Lisboa, Portugal

P. Bargassa, C. Beirão Da Cruz E Silva, B. Calpas, A. Di Francesco, P. Faccioli, M. Gallinaro, J. Hollar, N. Leonardo, L. Lloret Iglesias, M.V. Nemallapudi, J. Seixas, O. Toldaiev, D. Vadruccio, J. Varela

Joint Institute for Nuclear Research, Dubna, Russia

S. Afanasiev, P. Bunin, M. Gavrilenko, I. Golutvin, I. Gorbunov, A. Kamenev, V. Karjavin, A. Lanev, A. Malakhov, V. Matveev[37,38], V. Palichik, V. Perelygin, S. Shmatov, S. Shulha, N. Skatchkov, V. Smirnov, N. Voytishin, A. Zarubin

Petersburg Nuclear Physics Institute, Gatchina (St. Petersburg), Russia

L. Chtchipounov, V. Golovtsov, Y. Ivanov, V. Kim[39], E. Kuznetsova[40], V. Murzin, V. Oreshkin, V. Sulimov, A. Vorobyev

Institute for Nuclear Research, Moscow, Russia

Yu. Andreev, A. Dermenev, S. Gninenko, N. Golubev, A. Karneyeu, M. Kirsanov, N. Krasnikov, A. Pashenkov, D. Tlisov, A. Toropin

Institute for Theoretical and Experimental Physics, Moscow, Russia

V. Epshteyn, V. Gavrilov, N. Lychkovskaya, V. Popov, I. Pozdnyakov, G. Safronov, A. Spiridonov, M. Toms, E. Vlasov, A. Zhokin

Moscow Institute of Physics and Technology, Moscow, Russia

T. Aushev, A. Bylinkin[38]

National Research Nuclear University 'Moscow Engineering Physics Institute' (MEPhI), Moscow, Russia

R. Chistov[41], M. Danilov[41], E. Zhemchugov

P.N. Lebedev Physical Institute, Moscow, Russia

V. Andreev, M. Azarkin[38], I. Dremin[38], M. Kirakosyan, A. Leonidov[38], A. Terkulov

Skobeltsyn Institute of Nuclear Physics, Lomonosov Moscow State University, Moscow, Russia

A. Baskakov, A. Belyaev, E. Boos, M. Dubinin[42], L. Dudko, A. Ershov, A. Gribushin, V. Klyukhin, O. Kodolova, I. Lokhtin, I. Miagkov, S. Obraztsov, S. Petrushanko, V. Savrin, A. Snigirev

Novosibirsk State University (NSU), Novosibirsk, Russia

V. Blinov[43], Y.Skovpen[43], D. Shtol[43]

State Research Center of Russian Federation, Institute for High Energy Physics, Protvino, Russia

I. Azhgirey, I. Bayshev, S. Bitioukov, D. Elumakhov, V. Kachanov, A. Kalinin, D. Konstantinov, V. Krychkine, V. Petrov, R. Ryutin, A. Sobol, S. Troshin, N. Tyurin, A. Uzunian, A. Volkov

University of Belgrade, Faculty of Physics and Vinca Institute of Nuclear Sciences, Belgrade, Serbia

P. Adzic[44], P. Cirkovic, D. Devetak, M. Dordevic, J. Milosevic, V. Rekovic

Centro de Investigaciones Energéticas Medioambientales y Tecnológicas (CIEMAT), Madrid, Spain

J. Alcaraz Maestre, M. Barrio Luna, E. Calvo, M. Cerrada, M. Chamizo Llatas, N. Colino, B. De La Cruz, A. Delgado Peris, A. Escalante Del Valle, C. Fernandez Bedoya, J.P. Fernández Ramos, J. Flix, M.C. Fouz, P. Garcia-Abia, O. Gonzalez Lopez, S. Goy Lopez, J.M. Hernandez, M.I. Josa, E. Navarro De Martino, A. Pérez-Calero Yzquierdo, J. Puerta Pelayo, A. Quintario Olmeda, I. Redondo, L. Romero, M.S. Soares

Universidad Autónoma de Madrid, Madrid, Spain

J.F. de Trocóniz, M. Missiroli, D. Moran

Universidad de Oviedo, Oviedo, Spain

J. Cuevas, J. Fernandez Menendez, I. Gonzalez Caballero, J.R. González Fernández, E. Palencia Cortezon, S. Sanchez Cruz, I. Suárez Andrés, P. Vischia, J.M. Vizan Garcia

Instituto de Física de Cantabria (IFCA), CSIC-Universidad de Cantabria, Santander, Spain

I.J. Cabrillo, A. Calderon, E. Curras, M. Fernandez, J. Garcia-Ferrero, G. Gomez, A. Lopez Virto, J. Marco, C. Martinez Rivero, F. Matorras, J. Piedra Gomez, T. Rodrigo, A. Ruiz-Jimeno, L. Scodellaro, N. Trevisani, I. Vila, R. Vilar Cortabitarte

CERN, European Organization for Nuclear Research, Geneva, Switzerland

D. Abbaneo, E. Auffray, G. Auzinger, P. Baillon, A.H. Ball, D. Barney, P. Bloch, A. Bocci, C. Botta, T. Camporesi, R. Castello, M. Cepeda, G. Cerminara, Y. Chen, A. Cimmino, D. d'Enterria, A. Dabrowski, V. Daponte, A. David, M. De Gruttola, A. De Roeck, E. Di Marco[45], M. Dobson, B. Dorney, T. du Pree, D. Duggan, M. Dünser, N. Dupont, A. Elliott-Peisert, P. Everaerts, S. Fartoukh, G. Franzoni, J. Fulcher, W. Funk, D. Gigi, K. Gill, M. Girone, F. Glege, D. Gulhan, S. Gundacker, M. Guthoff, P. Harris, J. Hegeman, V. Innocente, P. Janot, J. Kieseler, H. Kirschenmann, V. Knünz, A. Kornmayer[16], M.J. Kortelainen, K. Kousouris, M. Krammer[1], C. Lange, P. Lecoq, C. Lourenço, M.T. Lucchini, L. Malgeri, M. Mannelli, A. Martelli, F. Meijers, J.A. Merlin, S. Mersi, E. Meschi, P. Milenovic[46], F. Moortgat, S. Morovic, M. Mulders, H. Neugebauer, S. Orfanelli, L. Orsini, L. Pape, E. Perez, M. Peruzzi, A. Petrilli, G. Petrucciani, A. Pfeiffer, M. Pierini, A. Racz, T. Reis, G. Rolandi[47], M. Rovere, H. Sakulin, J.B. Sauvan, C. Schäfer, C. Schwick, M. Seidel, A. Sharma, P. Silva, P. Sphicas[48], J. Steggemann, M. Stoye, Y. Takahashi, M. Tosi, D. Treille, A. Triossi, A. Tsirou, V. Veckalns[49], G.I. Veres[21], M. Verweij, N. Wardle, H.K. Wöhri, A. Zagozdzinska[36], W.D. Zeuner

Paul Scherrer Institut, Villigen, Switzerland

W. Bertl, K. Deiters, W. Erdmann, R. Horisberger, Q. Ingram, H.C. Kaestli, D. Kotlinski, U. Langenegger, T. Rohe, S.A. Wiederkehr

Institute for Particle Physics, ETH Zurich, Zurich, Switzerland

F. Bachmair, L. Bäni, L. Bianchini, B. Casal, G. Dissertori, M. Dittmar, M. Donegà, C. Grab, C. Heidegger, D. Hits, J. Hoss, G. Kasieczka, W. Lustermann, B. Mangano, M. Marionneau, P. Martinez Ruiz del Arbol, M. Masciovecchio, M.T. Meinhard, D. Meister, F. Micheli, P. Musella, F. Nessi-Tedaldi, F. Pandolfi, J. Pata, F. Pauss, G. Perrin, L. Perrozzi, M. Quittnat, M. Rossini, M. Schönenberger, A. Starodumov[50], V.R. Tavolaro, K. Theofilatos, R. Wallny

Universität Zürich, Zurich, Switzerland

T.K. Aarrestad, C. Amsler[51], L. Caminada, M.F. Canelli, A. De Cosa, C. Galloni, A. Hinzmann, T. Hreus, B. Kilminster, J. Ngadiuba, D. Pinna, G. Rauco, P. Robmann, D. Salerno, C. Seitz, Y. Yang, A. Zucchetta

National Central University, Chung-Li, Taiwan

V. Candelise, T.H. Doan, Sh. Jain, R. Khurana, M. Konyushikhin, C.M. Kuo, W. Lin, A. Pozdnyakov, S.S. Yu

National Taiwan University (NTU), Taipei, Taiwan

Arun Kumar, P. Chang, Y.H. Chang, Y. Chao, K.F. Chen, P.H. Chen, F. Fiori, W.-S. Hou, Y. Hsiung, Y.F. Liu, R.-S. Lu, M. Miñano Moya, E. Paganis, A. Psallidas, J.f. Tsai

Chulalongkorn University, Faculty of Science, Department of Physics, Bangkok, Thailand

B. Asavapibhop, G. Singh, N. Srimanobhas, N. Suwonjandee

Cukurova University - Physics Department, Science and Art Faculty

A. Adiguzel, S. Cerci[52], S. Damarseckin, Z.S. Demiroglu, C. Dozen, I. Dumanoglu, S. Girgis, G. Gokbulut, Y. Guler, I. Hos[53], E.E. Kangal[54], O. Kara, U. Kiminsu, M. Oglakci, G. Onengut[55], K. Ozdemir[56], D. Sunar Cerci[52], B. Tali[52], H. Topakli[57], S. Turkcapar, I.S. Zorbakir, C. Zorbilmez

Middle East Technical University, Physics Department, Ankara, Turkey

B. Bilin, S. Bilmis, B. Isildak[58], G. Karapinar[59], M. Yalvac, M. Zeyrek

Bogazici University, Istanbul, Turkey

E. Gülmez, M. Kaya[60], O. Kaya[61], E.A. Yetkin[62], T. Yetkin[63]

Istanbul Technical University, Istanbul, Turkey

A. Cakir, K. Cankocak, S. Sen[64]

Institute for Scintillation Materials of National Academy of Science of Ukraine, Kharkov, Ukraine

B. Grynyov

National Scientific Center, Kharkov Institute of Physics and Technology, Kharkov, Ukraine

L. Levchuk, P. Sorokin

University of Bristol, Bristol, United Kingdom

R. Aggleton, F. Ball, L. Beck, J.J. Brooke, D. Burns, E. Clement, D. Cussans, H. Flacher, J. Goldstein, M. Grimes, G.P. Heath, H.F. Heath, J. Jacob, L. Kreczko, C. Lucas, D.M. Newbold[65], S. Paramesvaran, A. Poll, T. Sakuma, S. Seif El Nasr-storey, D. Smith, V.J. Smith

Rutherford Appleton Laboratory, Didcot, United Kingdom

K.W. Bell, A. Belyaev[66], C. Brew, R.M. Brown, L. Calligaris, D. Cieri, D.J.A. Cockerill, J.A. Coughlan, K. Harder, S. Harper, E. Olaiya, D. Petyt, C.H. Shepherd-Themistocleous, A. Thea, I.R. Tomalin, T. Williams

Imperial College, London, United Kingdom

M. Baber, R. Bainbridge, O. Buchmuller, A. Bundock, D. Burton, S. Casasso, M. Citron, D. Colling, L. Corpe, P. Dauncey, G. Davies, A. De Wit, M. Della Negra, R. Di Maria, P. Dunne, A. Elwood, D. Futyan, Y. Haddad, G. Hall, G. Iles, T. James, R. Lane, C. Laner, R. Lucas[65], L. Lyons, A.-M. Magnan, S. Malik, L. Mastrolorenzo, J. Nash, A. Nikitenko[50], J. Pela, B. Penning, M. Pesaresi, D.M. Raymond, A. Richards, A. Rose, E. Scott, C. Seez, S. Summers, A. Tapper, K. Uchida, M. Vazquez Acosta[67], T. Virdee[16], J. Wright, S.C. Zenz

Brunel University, Uxbridge, United Kingdom

J.E. Cole, P.R. Hobson, A. Khan, P. Kyberd, I.D. Reid, P. Symonds, L. Teodorescu, M. Turner

Baylor University, Waco, U.S.A.

A. Borzou, K. Call, J. Dittmann, K. Hatakeyama, H. Liu, N. Pastika

Catholic University of America

R. Bartek, A. Dominguez

The University of Alabama, Tuscaloosa, U.S.A.

A. Buccilli, S.I. Cooper, C. Henderson, P. Rumerio, C. West

Boston University, Boston, U.S.A.

D. Arcaro, A. Avetisyan, T. Bose, D. Gastler, D. Rankin, C. Richardson, J. Rohlf, L. Sulak, D. Zou

Brown University, Providence, U.S.A.

G. Benelli, D. Cutts, A. Garabedian, J. Hakala, U. Heintz, J.M. Hogan, O. Jesus, K.H.M. Kwok, E. Laird, G. Landsberg, Z. Mao, M. Narain, S. Piperov, S. Sagir, E. Spencer, R. Syarif

University of California, Davis, Davis, U.S.A.

R. Breedon, D. Burns, M. Calderon De La Barca Sanchez, S. Chauhan, M. Chertok, J. Conway, R. Conway, P.T. Cox, R. Erbacher, C. Flores, G. Funk, M. Gardner, W. Ko, R. Lander, C. Mclean, M. Mulhearn, D. Pellett, J. Pilot, S. Shalhout, M. Shi, J. Smith, M. Squires, D. Stolp, K. Tos, M. Tripathi

University of California, Los Angeles, U.S.A.

M. Bachtis, C. Bravo, R. Cousins, A. Dasgupta, A. Florent, J. Hauser, M. Ignatenko, N. Mccoll, D. Saltzberg, C. Schnaible, V. Valuev, M. Weber

University of California, Riverside, Riverside, U.S.A.

E. Bouvier, K. Burt, R. Clare, J. Ellison, J.W. Gary, S.M.A. Ghiasi Shirazi, G. Hanson, J. Heilman, P. Jandir, E. Kennedy, F. Lacroix, O.R. Long, M. Olmedo Negrete, M.I. Paneva, A. Shrinivas, W. Si, H. Wei, S. Wimpenny, B. R. Yates

University of California, San Diego, La Jolla, U.S.A.

J.G. Branson, G.B. Cerati, S. Cittolin, M. Derdzinski, R. Gerosa, A. Holzner, D. Klein, V. Krutelyov, J. Letts, I. Macneill, D. Olivito, S. Padhi, M. Pieri, M. Sani, V. Sharma, S. Simon, M. Tadel, A. Vartak, S. Wasserbaech[68], C. Welke, J. Wood, F. Würthwein, A. Yagil, G. Zevi Della Porta

University of California, Santa Barbara - Department of Physics, Santa Barbara, U.S.A.

N. Amin, R. Bhandari, J. Bradmiller-Feld, C. Campagnari, A. Dishaw, V. Dutta, M. Franco Sevilla, C. George, F. Golf, L. Gouskos, J. Gran, R. Heller, J. Incandela, S.D. Mullin, A. Ovcharova, H. Qu, J. Richman, D. Stuart, I. Suarez, J. Yoo

California Institute of Technology, Pasadena, U.S.A.

D. Anderson, J. Bendavid, A. Bornheim, J. Bunn, J. Duarte, J.M. Lawhorn, A. Mott, H.B. Newman, C. Pena, M. Spiropulu, J.R. Vlimant, S. Xie, R.Y. Zhu

Carnegie Mellon University, Pittsburgh, U.S.A.

M.B. Andrews, T. Ferguson, M. Paulini, J. Russ, M. Sun, H. Vogel, I. Vorobiev, M. Weinberg

University of Colorado Boulder, Boulder, U.S.A.

J.P. Cumalat, W.T. Ford, F. Jensen, A. Johnson, M. Krohn, S. Leontsinis, T. Mulholland, K. Stenson, S.R. Wagner

Cornell University, Ithaca, U.S.A.

J. Alexander, J. Chaves, J. Chu, S. Dittmer, K. Mcdermott, N. Mirman, G. Nicolas Kaufman, J.R. Patterson, A. Rinkevicius, A. Ryd, L. Skinnari, L. Soffi, S.M. Tan, Z. Tao, J. Thom, J. Tucker, P. Wittich, M. Zientek

Fairfield University, Fairfield, U.S.A.

D. Winn

Fermi National Accelerator Laboratory, Batavia, U.S.A.

S. Abdullin, M. Albrow, G. Apollinari, A. Apresyan, S. Banerjee, L.A.T. Bauerdick, A. Beretvas, J. Berryhill, P.C. Bhat, G. Bolla, K. Burkett, J.N. Butler, H.W.K. Cheung, F. Chlebana, S. Cihangir†, M. Cremonesi, V.D. Elvira, I. Fisk, J. Freeman, E. Gottschalk, L. Gray, D. Green, S. Grünendahl, O. Gutsche, D. Hare, R.M. Harris, S. Hasegawa, J. Hirschauer, Z. Hu, B. Jayatilaka, S. Jindariani, M. Johnson, U. Joshi, B. Klima, B. Kreis, S. Lammel, J. Linacre, D. Lincoln, R. Lipton, M. Liu, T. Liu, R. Lopes De Sá, J. Lykken, K. Maeshima, N. Magini, J.M. Marraffino, S. Maruyama, D. Mason, P. McBride, P. Merkel, S. Mrenna, S. Nahn, V. O'Dell, K. Pedro, O. Prokofyev, G. Rakness, L. Ristori, E. Sexton-Kennedy, A. Soha, W.J. Spalding, L. Spiegel, S. Stoynev, J. Strait, N. Strobbe, L. Taylor, S. Tkaczyk, N.V. Tran, L. Uplegger, E.W. Vaandering, C. Vernieri, M. Verzocchi, R. Vidal, M. Wang, H.A. Weber, A. Whitbeck, Y. Wu

University of Florida, Gainesville, U.S.A.

D. Acosta, P. Avery, P. Bortignon, D. Bourilkov, A. Brinkerhoff, A. Carnes, M. Carver, D. Curry, S. Das, R.D. Field, I.K. Furic, J. Konigsberg, A. Korytov, J.F. Low, P. Ma, K. Matchev, H. Mei, G. Mitselmakher, D. Rank, L. Shchutska, D. Sperka, L. Thomas, J. Wang, S. Wang, J. Yelton

Florida International University, Miami, U.S.A.

S. Linn, P. Markowitz, G. Martinez, J.L. Rodriguez

Florida State University, Tallahassee, U.S.A.

A. Ackert, T. Adams, A. Askew, S. Bein, S. Hagopian, V. Hagopian, K.F. Johnson, T. Kolberg, T. Perry, H. Prosper, A. Santra, R. Yohay

Florida Institute of Technology, Melbourne, U.S.A.

M.M. Baarmand, V. Bhopatkar, S. Colafranceschi, M. Hohlmann, D. Noonan, T. Roy, F. Yumiceva

University of Illinois at Chicago (UIC), Chicago, U.S.A.

M.R. Adams, L. Apanasevich, D. Berry, R.R. Betts, I. Bucinskaite, R. Cavanaugh, X. Chen, O. Evdokimov, L. Gauthier, C.E. Gerber, D.A. Hangal, D.J. Hofman, K. Jung, J. Kamin, I.D. Sandoval Gonzalez, H. Trauger, N. Varelas, H. Wang, Z. Wu, M. Zakaria, J. Zhang

The University of Iowa, Iowa City, U.S.A.

B. Bilki[69], W. Clarida, K. Dilsiz, S. Durgut, R.P. Gandrajula, M. Haytmyradov, V. Khristenko, J.-P. Merlo, H. Mermerkaya[70], A. Mestvirishvili, A. Moeller, J. Nachtman, H. Ogul, Y. Onel, F. Ozok[71], A. Penzo, C. Snyder, E. Tiras, J. Wetzel, K. Yi

Johns Hopkins University, Baltimore, U.S.A.

B. Blumenfeld, A. Cocoros, N. Eminizer, D. Fehling, L. Feng, A.V. Gritsan, P. Maksimovic, J. Roskes, U. Sarica, M. Swartz, M. Xiao, C. You

The University of Kansas, Lawrence, U.S.A.

A. Al-bataineh, P. Baringer, A. Bean, S. Boren, J. Bowen, J. Castle, L. Forthomme, S. Khalil, A. Kropivnitskaya, D. Majumder, W. Mcbrayer, M. Murray, S. Sanders, R. Stringer, J.D. Tapia Takaki, Q. Wang

Kansas State University, Manhattan, U.S.A.

A. Ivanov, K. Kaadze, Y. Maravin, A. Mohammadi, L.K. Saini, N. Skhirtladze, S. Toda

Lawrence Livermore National Laboratory, Livermore, U.S.A.

F. Rebassoo, D. Wright

University of Maryland, College Park, U.S.A.

C. Anelli, A. Baden, O. Baron, A. Belloni, B. Calvert, S.C. Eno, C. Ferraioli, J.A. Gomez, N.J. Hadley, S. Jabeen, G.Y. Jeng, R.G. Kellogg, J. Kunkle, A.C. Mignerey, F. Ricci-Tam, Y.H. Shin, A. Skuja, M.B. Tonjes, S.C. Tonwar

Massachusetts Institute of Technology, Cambridge, U.S.A.

D. Abercrombie, B. Allen, A. Apyan, V. Azzolini, R. Barbieri, A. Baty, R. Bi, K. Bierwagen, S. Brandt, W. Busza, I.A. Cali, M. D'Alfonso, Z. Demiragli, G. Gomez Ceballos, M. Goncharov, D. Hsu, Y. Iiyama, G.M. Innocenti, M. Klute, D. Kovalskyi, K. Krajczar, Y.S. Lai, Y.-J. Lee, A. Levin, P.D. Luckey, B. Maier, A.C. Marini, C. Mcginn, C. Mironov, S. Narayanan, X. Niu, C. Paus, C. Roland, G. Roland, J. Salfeld-Nebgen, G.S.F. Stephans, K. Tatar, D. Velicanu, J. Wang, T.W. Wang, B. Wyslouch

University of Minnesota, Minneapolis, U.S.A.

A.C. Benvenuti, R.M. Chatterjee, A. Evans, P. Hansen, S. Kalafut, S.C. Kao, Y. Kubota, Z. Lesko, J. Mans, S. Nourbakhsh, N. Ruckstuhl, R. Rusack, N. Tambe, J. Turkewitz

University of Mississippi, Oxford, U.S.A.

J.G. Acosta, S. Oliveros

University of Nebraska-Lincoln, Lincoln, U.S.A.

E. Avdeeva, K. Bloom, D.R. Claes, C. Fangmeier, R. Gonzalez Suarez, R. Kamalieddin, I. Kravchenko, A. Malta Rodrigues, J. Monroy, J.E. Siado, G.R. Snow, B. Stieger

State University of New York at Buffalo, Buffalo, U.S.A.

M. Alyari, J. Dolen, A. Godshalk, C. Harrington, I. Iashvili, J. Kaisen, D. Nguyen, A. Parker, S. Rappoccio, B. Roozbahani

Northeastern University, Boston, U.S.A.

G. Alverson, E. Barberis, A. Hortiangtham, A. Massironi, D.M. Morse, D. Nash, T. Orimoto, R. Teixeira De Lima, D. Trocino, R.-J. Wang, D. Wood

Northwestern University, Evanston, U.S.A.

S. Bhattacharya, O. Charaf, K.A. Hahn, A. Kumar, N. Mucia, N. Odell, B. Pollack, M.H. Schmitt, K. Sung, M. Trovato, M. Velasco

University of Notre Dame, Notre Dame, U.S.A.

N. Dev, M. Hildreth, K. Hurtado Anampa, C. Jessop, D.J. Karmgard, N. Kellams, K. Lannon, N. Marinelli, F. Meng, C. Mueller, Y. Musienko[37], M. Planer, A. Reinsvold, R. Ruchti, N. Rupprecht, G. Smith, S. Taroni, M. Wayne, M. Wolf, A. Woodard

The Ohio State University, Columbus, U.S.A.

J. Alimena, L. Antonelli, B. Bylsma, L.S. Durkin, S. Flowers, B. Francis, A. Hart, C. Hill, W. Ji, B. Liu, W. Luo, D. Puigh, B.L. Winer, H.W. Wulsin

Princeton University, Princeton, U.S.A.

S. Cooperstein, O. Driga, P. Elmer, J. Hardenbrook, P. Hebda, D. Lange, J. Luo, D. Marlow, T. Medvedeva, K. Mei, I. Ojalvo, J. Olsen, C. Palmer, P. Piroué, D. Stickland, A. Svyatkovskiy, C. Tully

University of Puerto Rico, Mayaguez, U.S.A.

S. Malik

Purdue University, West Lafayette, U.S.A.

A. Barker, V.E. Barnes, S. Folgueras, L. Gutay, M.K. Jha, M. Jones, A.W. Jung, A. Khatiwada, D.H. Miller, N. Neumeister, J.F. Schulte, X. Shi, J. Sun, F. Wang, W. Xie

Purdue University Northwest, Hammond, U.S.A.

N. Parashar, J. Stupak

Rice University, Houston, U.S.A.

A. Adair, B. Akgun, Z. Chen, K.M. Ecklund, F.J.M. Geurts, M. Guilbaud, W. Li, B. Michlin, M. Northup, B.P. Padley, J. Roberts, J. Rorie, Z. Tu, J. Zabel

University of Rochester, Rochester, U.S.A.

B. Betchart, A. Bodek, P. de Barbaro, R. Demina, Y.t. Duh, T. Ferbel, M. Galanti, A. Garcia-Bellido, J. Han, O. Hindrichs, A. Khukhunaishvili, K.H. Lo, P. Tan, M. Verzetti

Rutgers, The State University of New Jersey, Piscataway, U.S.A.

A. Agapitos, J.P. Chou, Y. Gershtein, T.A. Gómez Espinosa, E. Halkiadakis, M. Heindl, E. Hughes, S. Kaplan, R. Kunnawalkam Elayavalli, S. Kyriacou, A. Lath, K. Nash, M. Osherson, H. Saka, S. Salur, S. Schnetzer, D. Sheffield, S. Somalwar, R. Stone, S. Thomas, P. Thomassen, M. Walker

University of Tennessee, Knoxville, U.S.A.

A.G. Delannoy, M. Foerster, J. Heideman, G. Riley, K. Rose, S. Spanier, K. Thapa

Texas A&M University, College Station, U.S.A.

O. Bouhali[72], A. Celik, M. Dalchenko, M. De Mattia, A. Delgado, S. Dildick, R. Eusebi, J. Gilmore, T. Huang, E. Juska, T. Kamon[73], R. Mueller, Y. Pakhotin, R. Patel, A. Perloff, L. Perniè, D. Rathjens, A. Safonov, A. Tatarinov, K.A. Ulmer

Texas Tech University, Lubbock, U.S.A.

N. Akchurin, J. Damgov, F. De Guio, C. Dragoiu, P.R. Dudero, J. Faulkner, E. Gurpinar, S. Kunori, K. Lamichhane, S.W. Lee, T. Libeiro, T. Peltola, S. Undleeb, I. Volobouev, Z. Wang

Vanderbilt University, Nashville, U.S.A.

S. Greene, A. Gurrola, R. Janjam, W. Johns, C. Maguire, A. Melo, H. Ni, P. Sheldon, S. Tuo, J. Velkovska, Q. Xu

University of Virginia, Charlottesville, U.S.A.

M.W. Arenton, P. Barria, B. Cox, J. Goodell, R. Hirosky, A. Ledovskoy, H. Li, C. Neu, T. Sinthuprasith, X. Sun, Y. Wang, E. Wolfe, F. Xia

Wayne State University, Detroit, U.S.A.

C. Clarke, R. Harr, P.E. Karchin, J. Sturdy, S. Zaleski

University of Wisconsin - Madison, Madison, WI, U.S.A.

D.A. Belknap, J. Buchanan, C. Caillol, S. Dasu, L. Dodd, S. Duric, B. Gomber, M. Grothe, M. Herndon, A. Hervé, U. Hussain, P. Klabbers, A. Lanaro, A. Levine, K. Long, R. Loveless, G.A. Pierro, G. Polese, T. Ruggles, A. Savin, N. Smith, W.H. Smith, D. Taylor, N. Woods

†: Deceased
1: Also at Vienna University of Technology, Vienna, Austria
2: Also at State Key Laboratory of Nuclear Physics and Technology, Peking University, Beijing, China
3: Also at Institut Pluridisciplinaire Hubert Curien (IPHC), Université de Strasbourg, CNRS/IN2P3, Strasbourg, France
4: Also at Universidade Estadual de Campinas, Campinas, Brazil
5: Also at Universidade Federal de Pelotas, Pelotas, Brazil
6: Also at Université Libre de Bruxelles, Bruxelles, Belgium
7: Also at Deutsches Elektronen-Synchrotron, Hamburg, Germany
8: Also at Universidad de Antioquia, Medellin, Colombia

9: Also at Joint Institute for Nuclear Research, Dubna, Russia

10: Also at Helwan University, Cairo, Egypt

11: Now at Zewail City of Science and Technology, Zewail, Egypt

12: Also at British University in Egypt, Cairo, Egypt

13: Now at Ain Shams University, Cairo, Egypt

14: Also at Université de Haute Alsace, Mulhouse, France

15: Also at Skobeltsyn Institute of Nuclear Physics, Lomonosov Moscow State University, Moscow, Russia

16: Also at CERN, European Organization for Nuclear Research, Geneva, Switzerland

17: Also at RWTH Aachen University, III. Physikalisches Institut A, Aachen, Germany

18: Also at University of Hamburg, Hamburg, Germany

19: Also at Brandenburg University of Technology, Cottbus, Germany

20: Also at Institute of Nuclear Research ATOMKI, Debrecen, Hungary

21: Also at MTA-ELTE Lendület CMS Particle and Nuclear Physics Group, Eötvös Loránd University, Budapest, Hungary

22: Also at Institute of Physics, University of Debrecen, Debrecen, Hungary

23: Also at Indian Institute of Technology Bhubaneswar, Bhubaneswar, India

24: Also at University of Visva-Bharati, Santiniketan, India

25: Also at Indian Institute of Science Education and Research, Bhopal, India

26: Also at Institute of Physics, Bhubaneswar, India

27: Also at University of Ruhuna, Matara, Sri Lanka

28: Also at Isfahan University of Technology, Isfahan, Iran

29: Also at Yazd University, Yazd, Iran

30: Also at Plasma Physics Research Center, Science and Research Branch, Islamic Azad University, Tehran, Iran

31: Also at Università degli Studi di Siena, Siena, Italy

32: Also at Purdue University, West Lafayette, U.S.A.

33: Also at International Islamic University of Malaysia, Kuala Lumpur, Malaysia

34: Also at Malaysian Nuclear Agency, MOSTI, Kajang, Malaysia

35: Also at Consejo Nacional de Ciencia y Tecnología, Mexico city, Mexico

36: Also at Warsaw University of Technology, Institute of Electronic Systems, Warsaw, Poland

37: Also at Institute for Nuclear Research, Moscow, Russia

38: Now at National Research Nuclear University 'Moscow Engineering Physics Institute' (MEPhI), Moscow, Russia

39: Also at St. Petersburg State Polytechnical University, St. Petersburg, Russia

40: Also at University of Florida, Gainesville, U.S.A.

41: Also at P.N. Lebedev Physical Institute, Moscow, Russia

42: Also at California Institute of Technology, Pasadena, U.S.A.

43: Also at Budker Institute of Nuclear Physics, Novosibirsk, Russia

44: Also at Faculty of Physics, University of Belgrade, Belgrade, Serbia

45: Also at INFN Sezione di Roma; Università di Roma, Roma, Italy

46: Also at University of Belgrade, Faculty of Physics and Vinca Institute of Nuclear Sciences, Belgrade, Serbia

47: Also at Scuola Normale e Sezione dell'INFN, Pisa, Italy

48: Also at National and Kapodistrian University of Athens, Athens, Greece

49: Also at Riga Technical University, Riga, Latvia

50: Also at Institute for Theoretical and Experimental Physics, Moscow, Russia

51: Also at Albert Einstein Center for Fundamental Physics, Bern, Switzerland

52: Also at Adiyaman University, Adiyaman, Turkey

53: Also at Istanbul Aydin University, Istanbul, Turkey

54: Also at Mersin University, Mersin, Turkey

55: Also at Cag University, Mersin, Turkey

56: Also at Piri Reis University, Istanbul, Turkey

57: Also at Gaziosmanpasa University, Tokat, Turkey

58: Also at Ozyegin University, Istanbul, Turkey

59: Also at Izmir Institute of Technology, Izmir, Turkey

60: Also at Marmara University, Istanbul, Turkey

61: Also at Kafkas University, Kars, Turkey

62: Also at Istanbul Bilgi University, Istanbul, Turkey

63: Also at Yildiz Technical University, Istanbul, Turkey

64: Also at Hacettepe University, Ankara, Turkey

65: Also at Rutherford Appleton Laboratory, Didcot, United Kingdom

66: Also at School of Physics and Astronomy, University of Southampton, Southampton, United Kingdom

67: Also at Instituto de Astrofísica de Canarias, La Laguna, Spain

68: Also at Utah Valley University, Orem, U.S.A.

69: Also at Argonne National Laboratory, Argonne, U.S.A.

70: Also at Erzincan University, Erzincan, Turkey

71: Also at Mimar Sinan University, Istanbul, Istanbul, Turkey

72: Also at Texas A&M University at Qatar, Doha, Qatar

73: Also at Kyungpook National University, Daegu, Korea